



King Saud University  
Saudi Pharmaceutical Journal

www.ksu.edu.sa  
www.sciencedirect.com



## ORIGINAL ARTICLE

# Investigation of the in vitro performance difference of drug-Soluplus<sup>®</sup> and drug-PEG 6000 dispersions when prepared using spray drying or lyophilization

Mohammad A. Altamimi <sup>a,b,\*</sup>, Steven H. Neau <sup>a</sup>

<sup>a</sup> Department of Pharmaceutical Sciences, Philadelphia College of Pharmacy, University of the Sciences, 600 S. 43rd Street, Philadelphia, PA 19104, United States

<sup>b</sup> Department of Pharmaceutics, College of Pharmacy, King Saud University, P.O. Box 2457, Riyadh 11451, Saudi Arabia

Received 23 March 2016; accepted 25 September 2016

## KEYWORDS

Spray drying;  
Lyophilization;  
Dissolution;  
Nifedipine;  
Sulfamethoxazole;  
Soluplus<sup>®</sup>;  
PEG 6000;  
Solid dispersion

**Abstract** Purpose: To evaluate the physicochemical and in vitro characteristics of solid dispersions using BCS II model drugs with Soluplus<sup>®</sup> and one of its component homopolymers, PEG 6000. Methods: Nifedipine (NIF) and sulfamethoxazole (SMX) of 99.3% and 99.5% purity, respectively, were selected as BCS II model drugs, such that an improved dissolution rate and concentration in the gastrointestinal tract should increase oral bioavailability. Soluplus<sup>®</sup> is an amorphous, tri-block, graft co-polymer with polyvinyl caprolactam, polyvinyl acetate, and polyethylene glycol (PCL: PVAc:PEG6000) in the ratio 57:30:13. PEG 6000 (BASF) is a waxy material with melting point of about 60 °C. Solid dispersions were prepared using lyophilization or spray drying techniques. Dissolution study, crystallinity content, and analysis for new chemical bond formation have been used to evaluate the dispersed materials. Results: Although each polymer improved the drug dissolution rate, dissolution from Soluplus<sup>®</sup> was slower. Enhanced dissolution rates were observed with NIF solid dispersions, but the dissolution profiles were quite different due to the selected technique, polymer, and dissolution medium. For SMX, there was similarity across the dissolution profiles despite the medium, polymer, or applied technique. Each polymer was able to maintain an elevated drug concentration over the three hour duration of the dissolution profile, i.e., supersaturation was supported by the polymer. DSC thermograms revealed no melting endotherm, suggesting that the drug is amorphous or molecularly dispersed. Conclusion: NIF and SMX solid dispersions were successfully prepared by spray drying and lyophilization using Soluplus<sup>®</sup> or PEG 6000. Each polymer enhanced the drug dissolution rate; NIF dissolution rate was improved to a greater extent.

\* Corresponding author at: Department of Pharmaceutics, College of Pharmacy, King Saud University, P.O. Box 2457, Riyadh 11451, Saudi Arabia.

E-mail address: [maltamimi@ksu.edu.sa](mailto:maltamimi@ksu.edu.sa) (M.A. Altamimi).

Peer review under responsibility of King Saud University.



Production and hosting by Elsevier

<http://dx.doi.org/10.1016/j.jsps.2016.09.013>

1319-0164 © 2016 The Authors. Production and hosting by Elsevier B.V. on behalf of King Saud University.

This is an open access article under the CC BY-NC-ND license (<http://creativecommons.org/licenses/by-nc-nd/4.0/>).

Please cite this article in press as: Altamimi, M.A., Neau, S.H. Investigation of the in vitro performance difference of drug-Soluplus<sup>®</sup> and drug-PEG 6000 dispersions when prepared using spray drying or lyophilization. Saudi Pharmaceutical Journal (2016), <http://dx.doi.org/10.1016/j.jsps.2016.09.013>

Dispersions with PEG 6000 had a faster dissolution rate due to its hydrophilic nature. DSC analysis showed that no crystalline material exists in the dispersions.

© 2016 The Authors. Production and hosting by Elsevier B.V. on behalf of King Saud University. This is an open access article under the CC BY-NC-ND license (<http://creativecommons.org/licenses/by-nc-nd/4.0/>).

## 1. Introduction

Most new chemical entities in the pharmaceutical industry lack the sufficient solubility in water (Fouad et al., 2011; Al-Obaidi and Buckton, 2009; Ning et al., 2011; Emara et al., 2002) and, thus, exhibit a slow dissolution rate and low oral bioavailability. This conundrum drives scientists to develop new strategies to overcome the repercussions of poor solubility. Enhancing the solubility of different chemical substances by forming a solid dispersion with a hydrophilic polymer is one of the most promising methods. Different hydrophilic polymers have been successfully used to enhance oral bioavailability by either enhancing the dissolution rate and/or increasing the drug concentration in the aqueous medium (Emara et al., 2002; Tanno et al., 2004; Konno et al., 2008).

Such solid dispersions also demonstrate an ability to maintain the amorphous state of a given drug during processing and storage. The amorphous form of a drug has a 10–1000 fold higher solubility than the crystalline form (Lakshman et al., 2008). Keeping this amorphous state, in part, is a function of drug concentration in the dispersion, indicating that some of the drug will recrystallize after exceeding a particular drug-polymer ratio (Weuts et al., 2011).

Polymers can possess different chemical and physical characteristics, such as functional groups, molecular weight, melting temperature  $T_m$ , and glass transition temperature  $T_g$ . Therefore, each polymer has a different ability to maintain dispersed drug at a particular drug-carrier ratio without recrystallization (Mahieu et al., 2012).

An approach to understand drug-carrier relationship in a solid dispersion took advantage of the thermodynamics described by the Flory-Huggins Theory (Marsac et al., 2006, 2009). From this theory, a prediction of the polymer saturation is calculated and proved to show promising results.

Sulfamethoxazole and nifedipine are the selected drug candidates for this study. The two drugs have a limited dissolution rate due to lower solubility. However, forming a complex or dispersing the drug in a hydrophilic carrier can often improve the dissolution rate (Emara et al., 2002; Özdemir and Erkin, 2012).

In our previous experiments, the saturation limits of these drugs in Soluplus® and its component homopolymers were investigated. PEG 6000 was found to exhibit a profound

impact on the reduction in the SMX and NIF melting endotherm (Altamimi and Neau, 2016). Polyvinyl caprolactam (PCL) and polyvinyl acetate (PVAc) showed essentially no reduction in the melting endotherm. Both polymers, also, proved to be practically difficult to process due to their hydrophobic nature (data not shown). Therefore, PVAc and PCL were excluded from this study.

In this study, Soluplus® as a parent polymer and one of its component homopolymers, PEG 6000, are assessed for their ability to form a solid dispersion by two different manufacturing techniques, spray drying and lyophilization, as they are the methods often used to produce solid dispersions. Stability, morphology, in vitro release profile, and the release kinetics of the dispersed materials are investigated.

## 2. Materials

Crystalline sulfamethoxazole (Fig. 1b) (SMX,  $M_w = 253.28$  g/mol, density =  $1.42$  g/cm<sup>3</sup>) was purchased from Flavine International Inc., Closter, NJ. Crystalline nifedipine (Fig. 1a) (NIF,  $M_w = 346.34$  g/mol, density =  $1.34$  g/cm<sup>3</sup>) was purchased from C.F.M. Co. Farmaceutica Milanese S.P.A. (Milano, Italia). Soluplus® (Fig. 1d) ( $M_w = 118,000$  g/mol, density =  $1.08$  g/cm<sup>3</sup>) and PEG 6000 (Fig. 1c) ( $M_w = 6000$  g/mol, density =  $1.08$  g/cm<sup>3</sup>) were generous gifts from BASF (Tarrytown, NY). Other properties of these materials are presented in Table 1.

## 3. Methods

### 3.1. Preparation of a solid dispersion

#### 3.1.1. Spray drying

Sulfamethoxazole and nifedipine with each polymer were prepared in drug:polymer mass ratios of 1:1, 1:5, and 1:9. Each drug with Soluplus® or PEG 6000, at the selected mass ratio, was dissolved in 250 ml of water/acetonitrile (1:5). Such solvent ratio was chosen after extensive experimentations to ensure using the same solution across the two preparation techniques. A magnetic bar was used to stir the mixture until a clear solution was observed. The solution was spray-dried using a Mini Spray-Dryer B-290 (Büchi Labortechnik AG, Flawil, Switzerland). The air flow was set to be 40 m<sup>3</sup>/h. For Soluplus® mixtures,

**Table 1** Material properties.

	$M_w$ (g/mol)	Density (g/cm <sup>3</sup> ) <sup>a</sup>	Molar volume (cm <sup>3</sup> /mol)	$\Delta H_{fus}$ (kJ/mol)	$T_m$ (K)	$T_g$ (K)
Sulfamethoxazole	253	1.42	172.3	28.7	443	289 <sup>b</sup>
Nifedipine	346	1.34	288.6	36.5	447	316
Soluplus®	118,000	1.08	109,000	–	–	347
PEG	6000	1.08	5555.6	1072	333	235

<sup>a</sup> True density, measured using helium pycnometry.

<sup>b</sup> Reference Baird et al. (2010) and Mahlin and Bergström (2013).

the solution was sprayed with an inlet air temperature of 90 °C and a flow rate of 25%. For PEG 6000 mixtures, the inlet temperature was 60 °C with a flow rate of 20%.

### 3.1.2. Lyophilization

Sulfamethoxazole and nifedipine with each polymer were prepared in drug:polymer mass ratios of 1:1, 1:5, and 1:9. Each drug with Soluplus® or PEG 6000, at the selected mass ratio, was dissolved in 250 ml of water/acetonitrile (1:5). A magnetic bar was used to stir the mixture until a clear solution was observed. The solution was placed in a −80 °C freezer for 24 h. The frozen solutions were then placed in an AdVantage XL-70 freeze dryer (Virtis, Gardiner, NY) at a condenser temperature of −60 °C and reduced pressure of 20 mbar for at least 24 h. The shelf temperature was −40 °C in the first day for primary drying. The lyophilized mixtures were taken from the lyophilizer and placed in a desiccator at 25 °C the following day for secondary drying.

### 3.2. Differential scanning calorimetry

Thermal analysis was conducted using a TA 2910 DSC (TA Instruments, New Castle, DE, USA) at a scan rate of 10 °C/min. Samples of 3–7 mg were weighed and placed in an aluminum pan and an aluminum lid was crimped to form a hermetic seal. The DSC was calibrated for temperature and enthalpy with indium (100% pure, melting point 156.60 °C, heat of fusion 6.80 cal/g). The sample and reference cells were purged with nitrogen at 50 ml/min. The results were analyzed using Thermal Advantage 1.1 A software.

### 3.3. Fourier transform infrared spectroscopy

The infrared spectrum of the drugs, the polymers, and their spray-dried and lyophilized mixtures were obtained using a Nicolet iS10 Fourier transform infrared (FTIR) spectrometer (Thermo Fisher Scientific, Madison, WI, USA). The materials were prepared as KBr pellets and spectra were collected across 4000–600 cm<sup>−1</sup> wave number using 64 scans and 2 cm<sup>−1</sup> resolution (Tanno et al., 2004; Sathigari et al., 2012).

### 3.4. Drug dissolution studies

#### 3.4.1. Dissolution tests

In vitro dissolution tests of SMX, NIF, and solid dispersions were conducted in 900 ml of SGF or SIF at 37.0 ± 0.2 °C using a Distek model 2100C (Distek, North Brunswick, NJ) with paddle rotation of 100 rpm. At designated time points, samples were drawn and filtered through a 0.45 µm in-line filter using a Distek model 2230A autosampler, and then analyzed using UV spectrophotometry at 260 and 240 nm for SMX and NIF, respectively. Each experiment was conducted at least in triplicate (Tao et al., 2009).

#### 3.4.2. Data analysis of release data

**3.4.2.1. Mathematical models of release kinetics.** Drug-polymer mixture release kinetics were evaluated using zero-order, first-order, Hixson-Crowell, Higuchi, and Ritger-Peppas model equations (Khan et al., 2012; Shoaib et al., 2006; Costa and Sousa Lobo, 2001).

**3.4.2.1.1. Zero-order kinetic model.** If a plot of the cumulative amount of drug released as a function of release time presents linear data, zero-order kinetics is suggested and the release rate is independent of the drug concentration.

$$\frac{M_t}{M_\infty} = M_o + k_o t \quad (1)$$

where  $M_o$ ,  $M_t$ , and  $M_\infty$  are the amount of drug released at the beginning, at time  $t$  in the release period, and the total mass of drug released at infinite time (typically taken to be the mass of drug available in the sample), respectively. The coefficient  $k_o$  is the zero order rate constant.

**3.4.2.1.2. First-order kinetic model.** If a plot of the negative of the log (base e) of 1 minus the cumulative fraction of drug released versus time is linear, drug is said to undergo first-order release. Eq. (2) shows the dependence of the release rate on the drug concentration.

$$-\ln \left( 1 - \frac{M_t}{M_\infty} \right) = k_1 t \quad (2)$$

**3.4.2.1.3. Higuchi kinetic model.** Plotting the cumulative amount of the released drug as a function of the square root of the release time renders linearized data if the drug is released by kinetics described by the Higuchi model. The model was developed to describe drug release from a matrix that remains intact during drug release:

$$\frac{M_t}{M_\infty} = M_o + k_H \sqrt{t} \quad (3)$$

where  $k_H$  is the Higuchi rate constant.

**3.4.2.1.4. Hixson-Crowell kinetic model.** The Hixson-Crowell kinetic model applies if a plot of the difference between the cube root of the mass of drug initially in a matrix, i.e.,  $M_\infty$ , and the cube root of the mass of drug remaining in that matrix at time  $t$ ,  $M_\infty - M_t$ , as a function of release time presents linearized data. The model describes drug release from a spherical matrix that erodes or dissolves proportionally across its surface area over time to release the drug.

$$(M_\infty)^{1/3} - (M_\infty - M_t)^{1/3} = k_{HC} t \quad (4)$$

$k_{HC}$  is the Hixson-Crowell rate constant.

**3.4.2.1.5. Ritger-Peppas kinetic model.** The plot for this kinetic model presents the fraction of drug released from the solid dosage form as a function of release time.

$$\frac{M_t}{M_\infty} = k_{RP} t^n \quad (5)$$

where  $k_{RP}$  is the Ritger-Peppas rate constant. The exponent,  $n$ , can provide some insight into the release mechanism, with dissolved drug diffusion from an essentially intact matrix at its low value (typically about 0.5) and polymer relaxation (hydration, swelling, and possibly gelling of the polymer) at the high extreme (typically about 1.0). At values between these extremes, the release mechanism is described as anomalous, indicating that drug release is achieved by a combination of mechanisms or by an undefined mechanism.

**3.4.2.2. Analysis of the drug release data.** Sigma Plot 2002 for Windows, version 12.0 (SPSS, Inc., Chicago, IL) was used to analyze and fit equations to the release data. The variables were predicted and  $p < 0.05$  was considered significant (Huang et al., 2006).

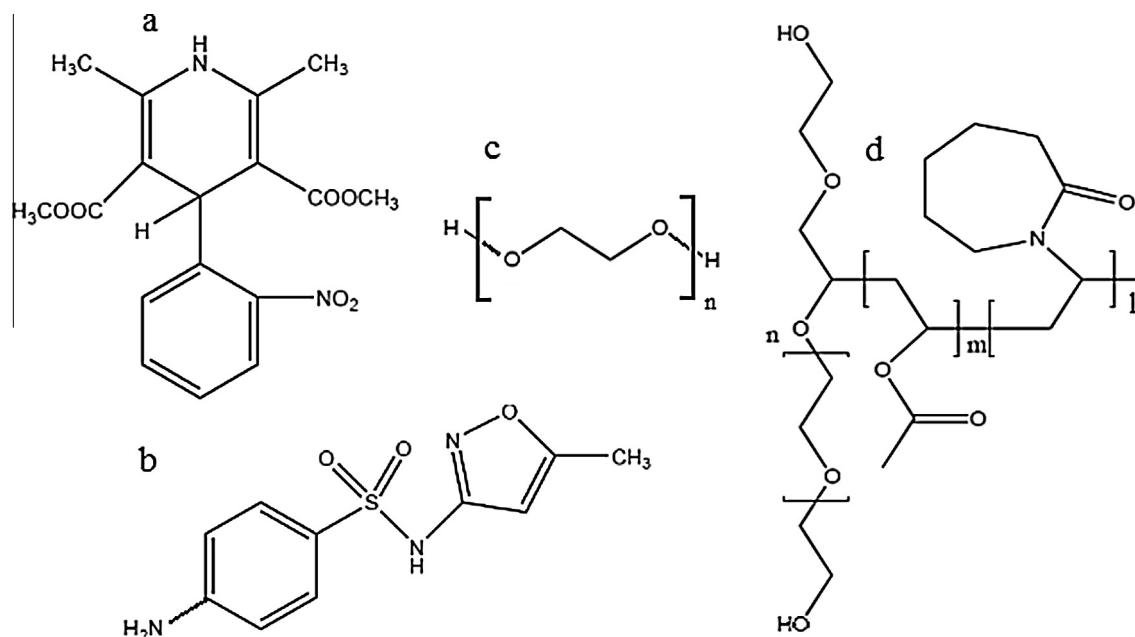


**Figure 1** Chemical structures of a. nifedipine, b. sulfamethoxazole, c. polyethylene glycol, and d. Soluplus®.

**3.4.2.3. Comparison of release profiles.** To evaluate the similarity of in vitro release profiles before and after the stability study, the similarity factor,  $f_2$ , will be calculated. The similarity factor, as defined in Eq. (6) is based on the difference in drug percent dissolved between the test and the reference product at specific time points:

$$f_2 = 50 * \log \left\{ \left( 1 + \left( \frac{1}{n} \right) \sum_{i=1}^n |R_i - T_i|^2 \right)^{-0.5} * 100 \right\} \quad (6)$$

where  $n$  is the number of time points,  $R_i$  is the percentage of drug released from the reference product, and  $T_i$  is the percentage released from the comparison product at different time points. The  $f_2$  value is 50–100 for similarity and less than 50 for dissimilarity in the dissolution profiles (Ning et al., 2011; Costa and Sousa Lobo, 2001; Flanner, 1996).

### 3.5. Drug stability studies

#### 3.5.1. Storage conditions for stability studies

Pure drug, pure polymer, and solid dispersions will be stored under 50 °C/0% RH and 25 °C/0% RH conditions. Thermal analysis was conducted after six months by DSC to evaluate the degree of crystallinity of the drug following each storage condition (Tanno et al., 2004).

## 4. Results and discussions

### 4.1. Differential scanning calorimetry

The melting endotherm of each drug and polymer is found in Fig. 2. Sulfamethoxazole has a melting point of 169.87 °C, nifedipine has a melting point of 173.05 °C, Soluplus® has a  $T_g$  around 70 °C, and PEG 6000 is semi crystalline with  $T_g$  around –22 °C (not shown in the figure) and a melting point of 60 °C.

#### 4.1.1. Spray dried solid dispersion

The DSC analysis for SMX-Soluplus® at different ratios is found in Fig. 3a. The melting endotherm for SMX is 169.9 °C; however, no melting endotherm was evident at any drug-polymer ratio in this experiment. This analysis proves that Soluplus®, even at a 1:1 mass ratio, successfully dispersed SMX with no trace of crystallinity when spray drying method was used. The  $T_g$  for the dispersed mixtures is shifting toward the original glass transition temperature of neat Soluplus® as the polymer content increases. This shift reveals an effective interaction between the drug and the polymer. Such a change in  $T_g$  indicates that the drug works as a plasticizer (Nagy et al., 2012). Gordon-Taylor (G-T) and Fox equations have been developed to predict the glass transition temperature of blends. However, the experimental  $T_g$  deviates from the  $T_g$  predicted by these equations. Such deviation is attributed to non-ideal mixing due to an unexpected change in volume (Weuts et al., 2011; Sathigari et al., 2012; Witold et al., 2008; Forster et al., 2001). Andronis et al., showed that an increase in moisture content substantially reduced the glass transition temperature of indomethacin (Vlassios Andronis and George, 1996). The moisture uptake was larger for the amorphous form of the drug. A significant reduction in the crystallization temperature as the moisture content increased is reported (Grisedale et al., 2012). In this work, focus is on the appearance of the melting endotherm at different polymer ratios. Each of the preparation methods renders dispersed materials with different moisture contents. However, it has been reported that the freeze drying method might induce drug crystallization. Such induction happens during the freezing step. In that step the solution will not freeze instantaneously allowing the water to form crystals. Finally, the sample freezes as a material that is amorphous, crystalline, or a combination of the two. The percentage of the solvent that does not freeze is considered bound solvent (Abdelwahed et al., 2006). In the literature, however, both methods, demonstrated a moisture content of up to 5% (Maa et al., 1998).

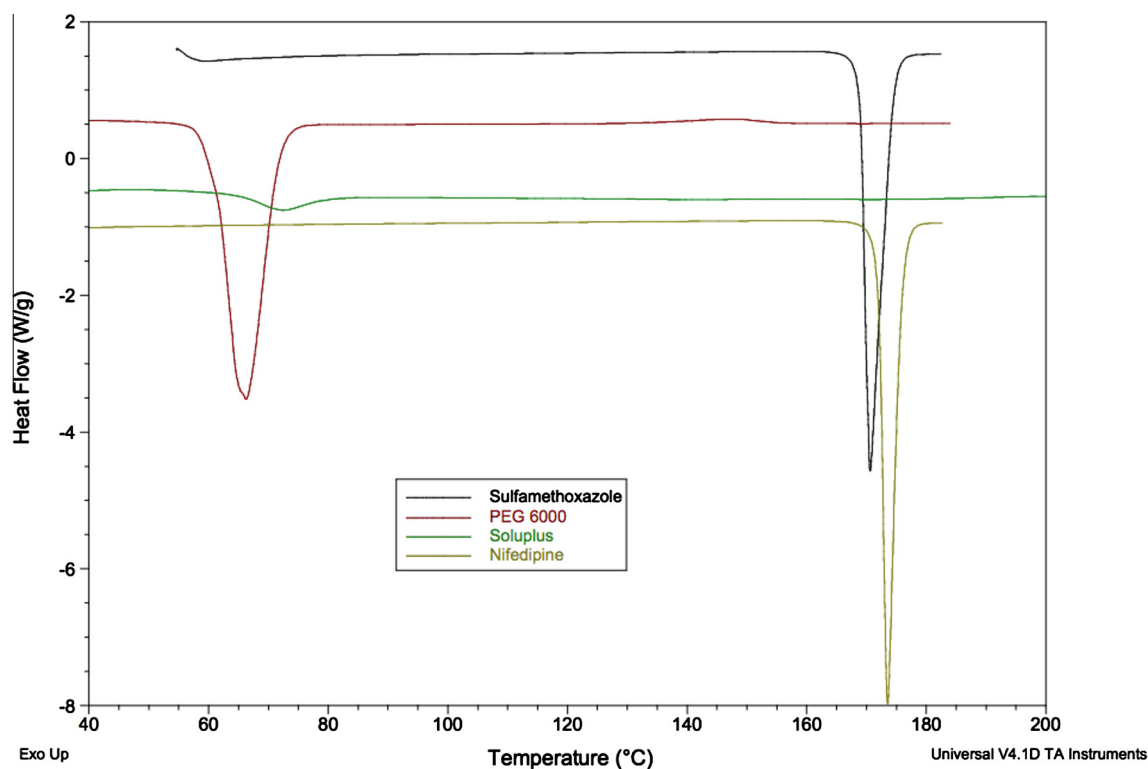


**Figure 2** DSC thermograms for (top to bottom) sulfamethoxazole, PEG 6000, Soluplus®, and nifedipine.

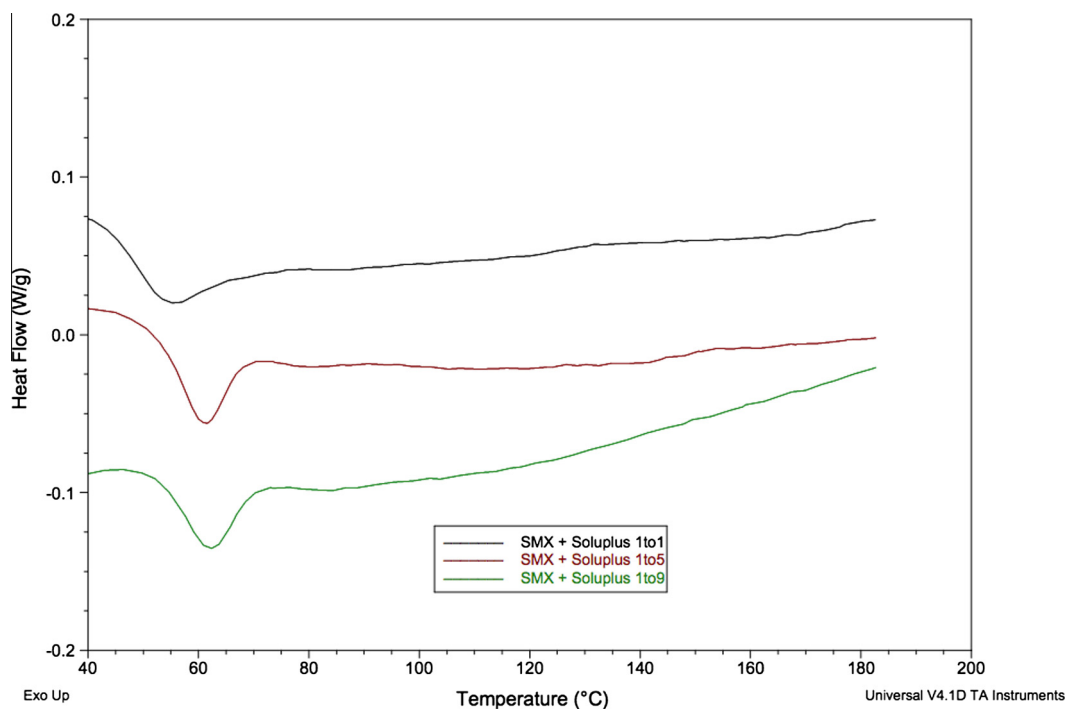


**Figure 3a** DSC thermograms of sulfamethoxazole:Soluplus® spray dried mixtures at a mass ratio of 1:1, 1:5, and 1:9.

DSC analysis for the SMX-PEG 6000 dispersions prepared using spray drying is found in Fig. 3b. The melting endotherm of PEG 6000 was around 57 °C, whereas no melting endotherm was found for SMX. It is obvious that the large melting

endotherm of PEG 6000 in the mixture enlarges the y-axis and, thus, obscures any melting endotherm for SMX at higher temperatures. However, there was no melting endotherm for SMX at temperature ranging from 75 to 160 °C.



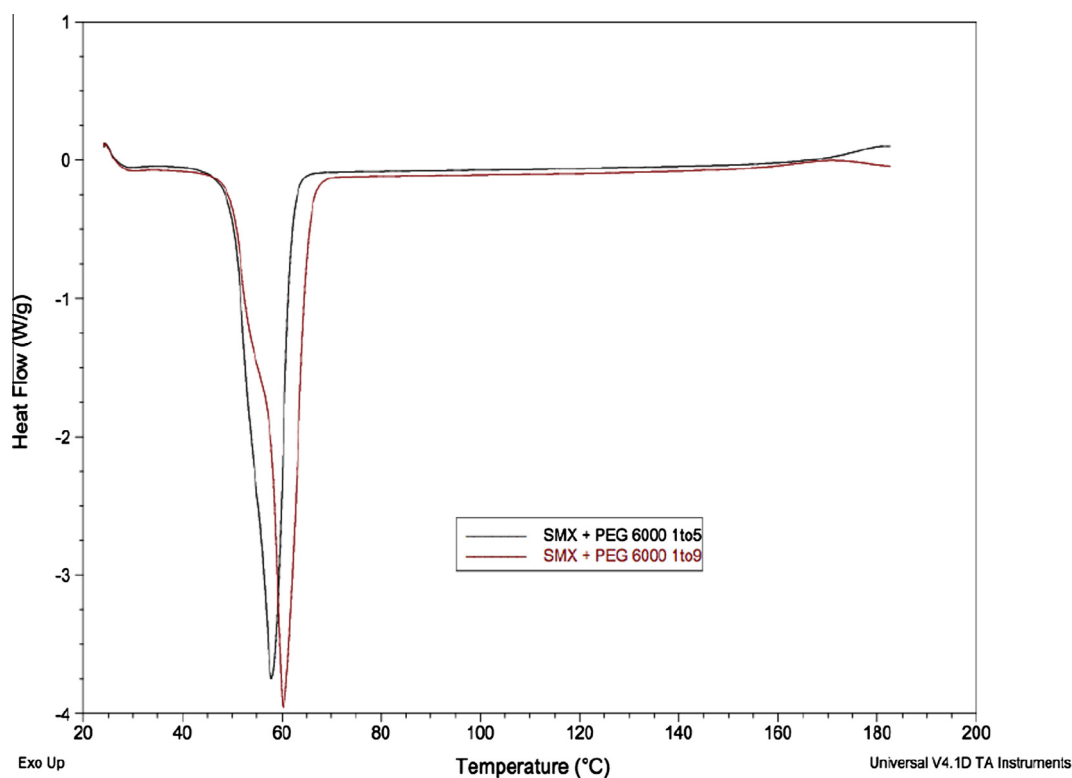


**Figure 3b** DSC thermograms of sulfamethoxazole:PEG 6000 spray dried mixtures at mass ratios of 1:5 and 1:9.

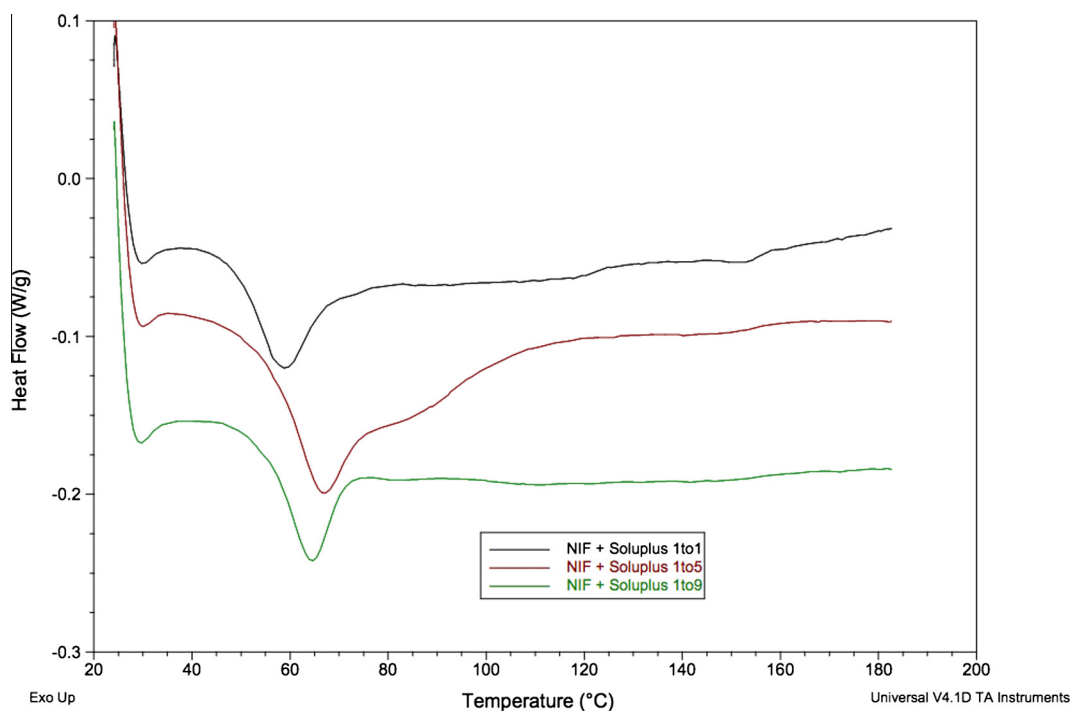


**Figure 4a** DSC thermograms of nifedipine:Soluplus® spray dried mixtures at mass ratios of 1:1, 1:5, and 1:9.

When the drug dissolves in the polymer and forms a solid solution, or when drug is dispersed in the polymer carrier as amorphous material, no drug melting endotherm can be detected. The slight change in PEG 6000 melting might be attrib-

uted to the dispersed drug or residual moisture effect. In addition, PEG 6000 exists in an extended or folded form. The latter will render a shoulder that precedes the melting of the extended form of the polymer (Corrigan et al., 2002). This shoulder is

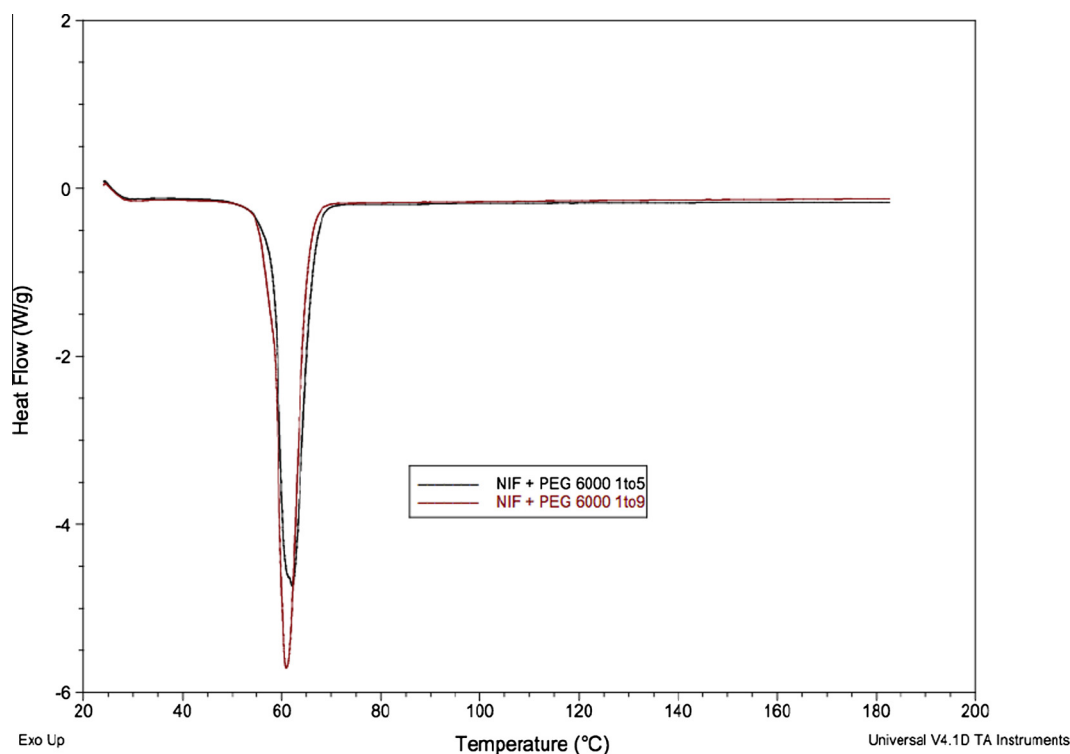


**Figure 4b** DSC thermograms for nifedipine:PEG 6000 spray dried mixtures at mass ratios of 1:5, and 1:9.

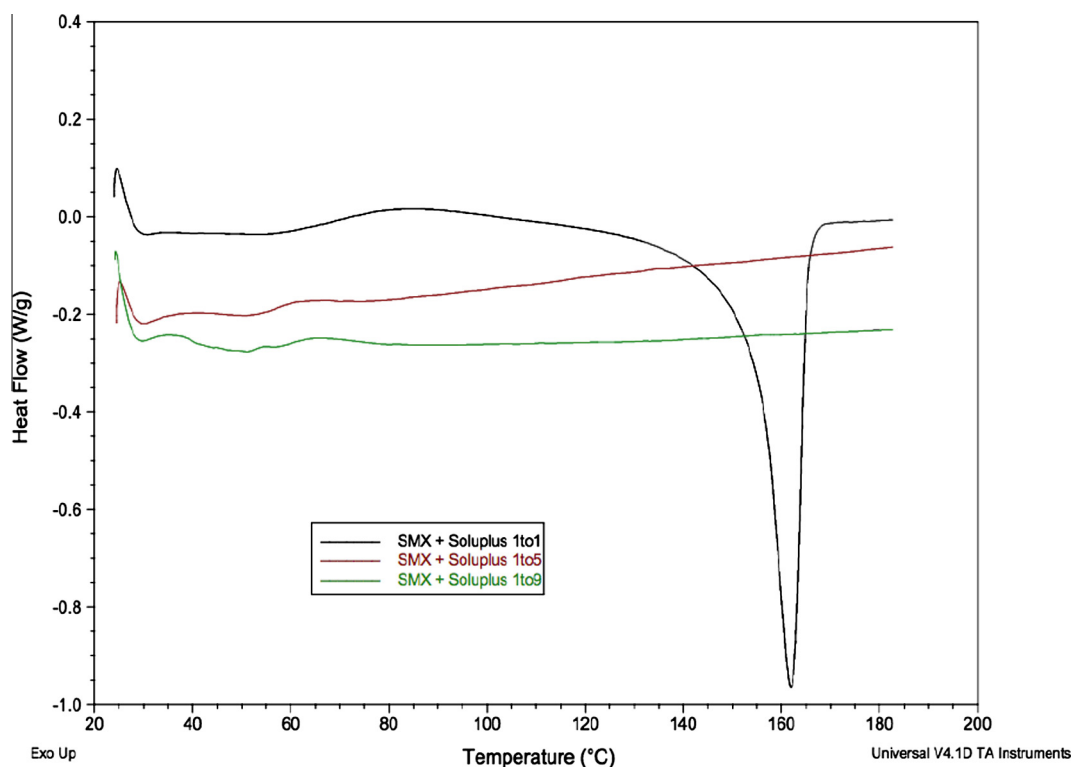


**Figure 5a** DSC thermograms for sulfamethoxazole:Soluplus<sup>®</sup> lyophilized mixtures at mass ratios of 1:1, 1:5, and 1:9.

attributed to the polymer chains that have folded during drying. Observed broad peaks at temperatures above 160 °C have been reported elsewhere (Fouad et al., 2011; Guyot et al., 1995). The

collected materials for 1:1 ratio were excluded. The material was sticking to the walls with high solvent content, unlike the other formulation where fine dry powder was collected.

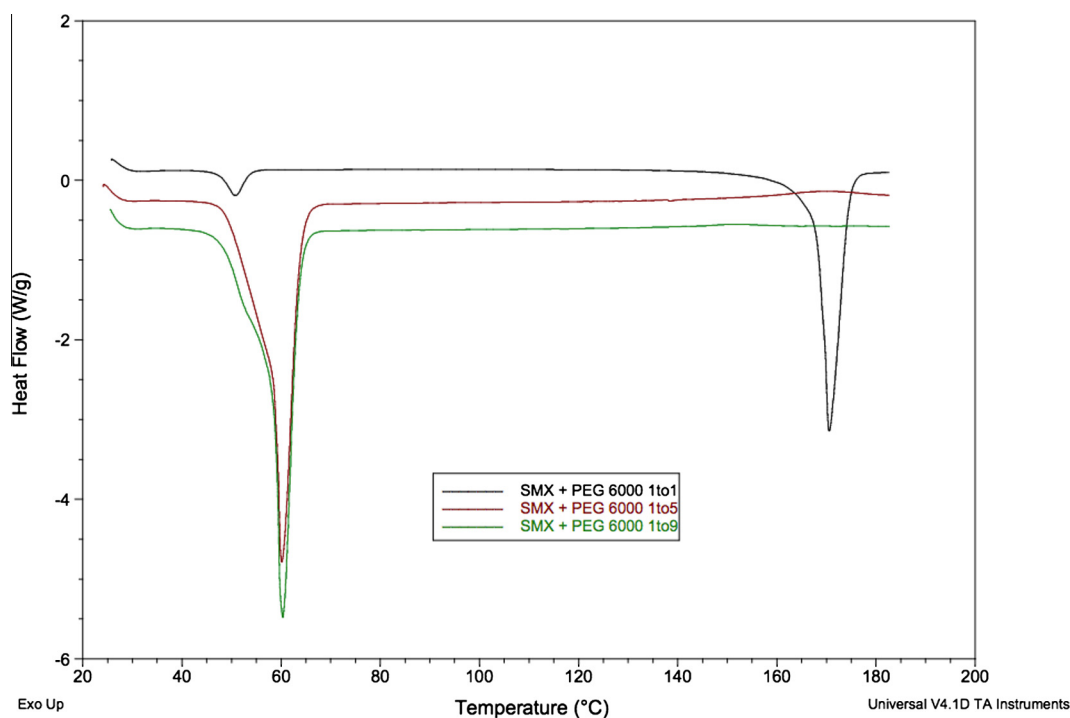


**Figure 5b** DSC thermograms for the sulfamethoxazole:PEG 6000 lyophilized mixtures at mass ratios of 1:1, 1:5, and 1:9.

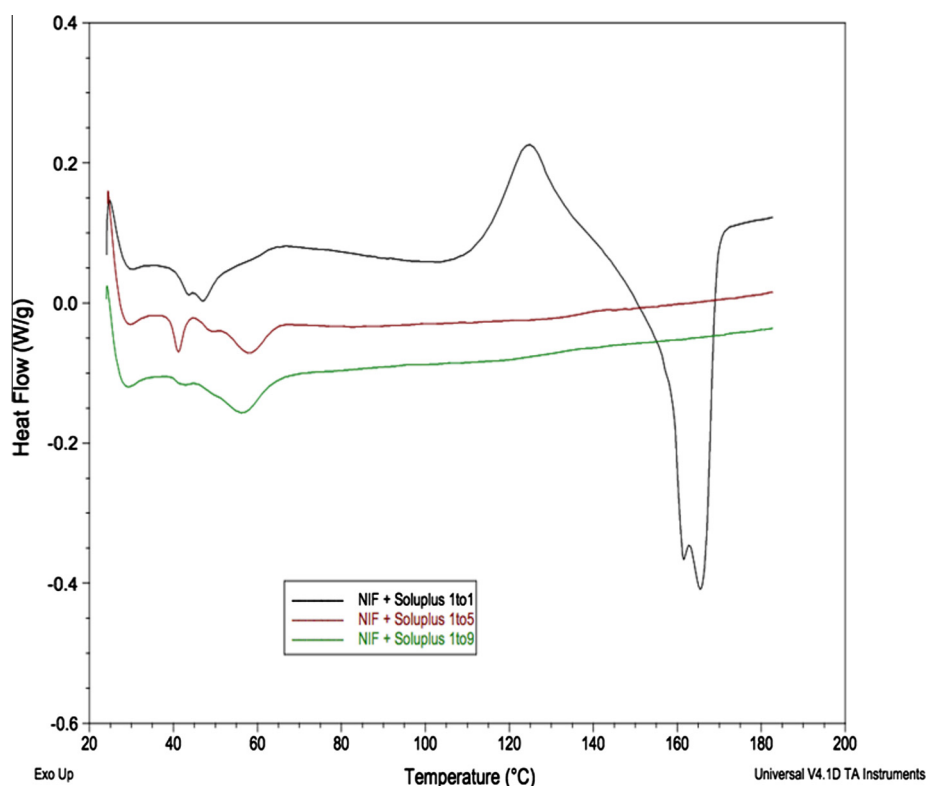


**Figure 6a** DSC thermograms for the nifedipine:Soluplus<sup>®</sup> lyophilized mixtures at mass ratios of 1:1, 1:5, and 1:9.

Thermal analyses of spray dried NIF-Soluplus<sup>®</sup> samples are found in Fig. 4a. A sharp melting endotherm was not found at any mass ratio. Negligible endothermic events were found in the thermograms for the mixtures at 1:1 and 1:5 mass

ratios that might be due to traces of crystalline NIF that did not dissolve in the polymer. An increase in the glass transition temperature with higher polymer ratios was observed, with a similar trend found for SMX-Soluplus<sup>®</sup> mixtures. SMX and



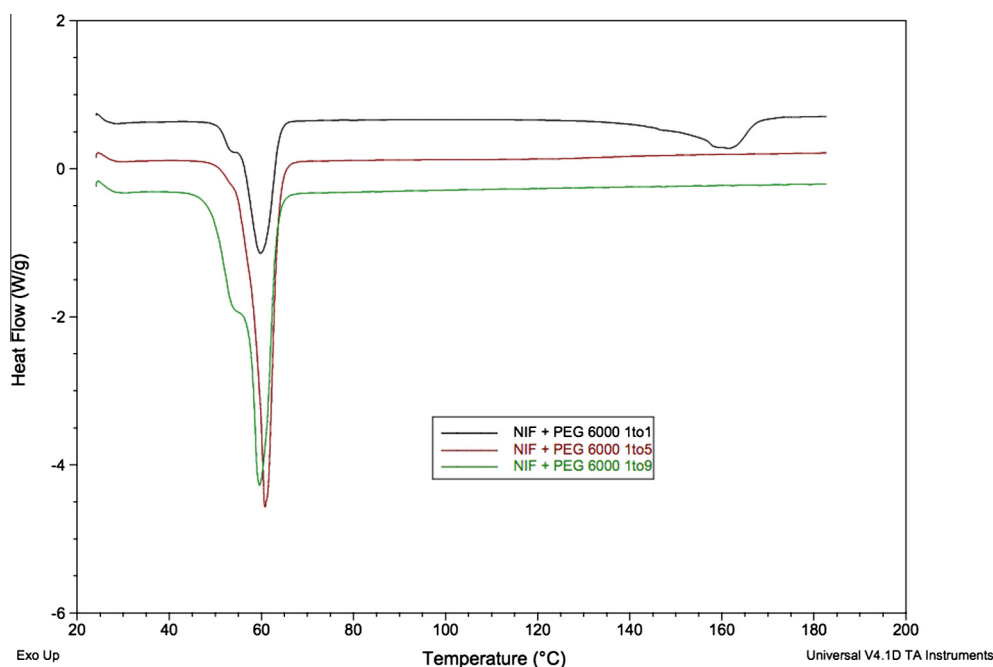


**Figure 6b** DSC thermograms for nifedipine:PEG 6000 lyophilized mixtures at mass ratios of 1:1, 1:5, and 1:9.

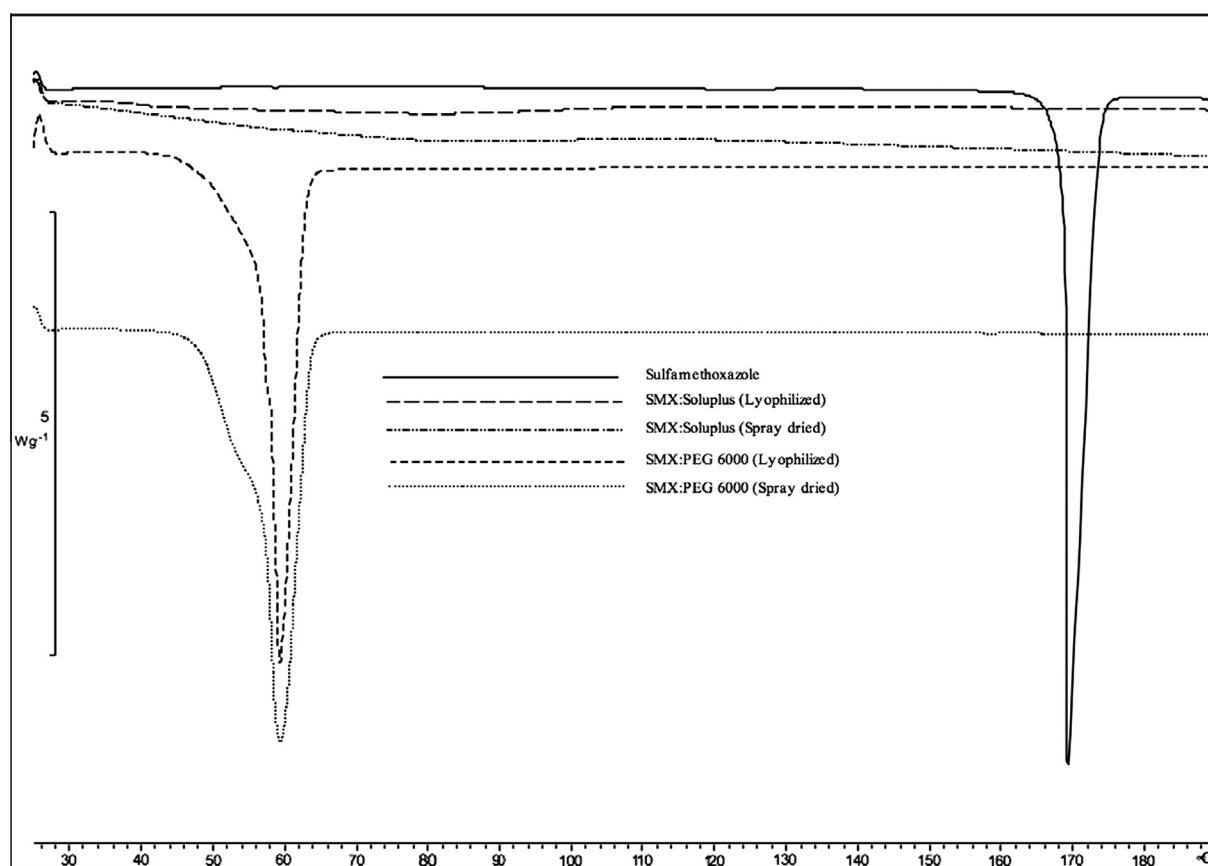


**Figure 7a** DSC thermograms for SMX mixtures with Soluplus® and with PEG 6000 at a mass ratio of 1:9 stored for six months at 0% RH and 25 °C.

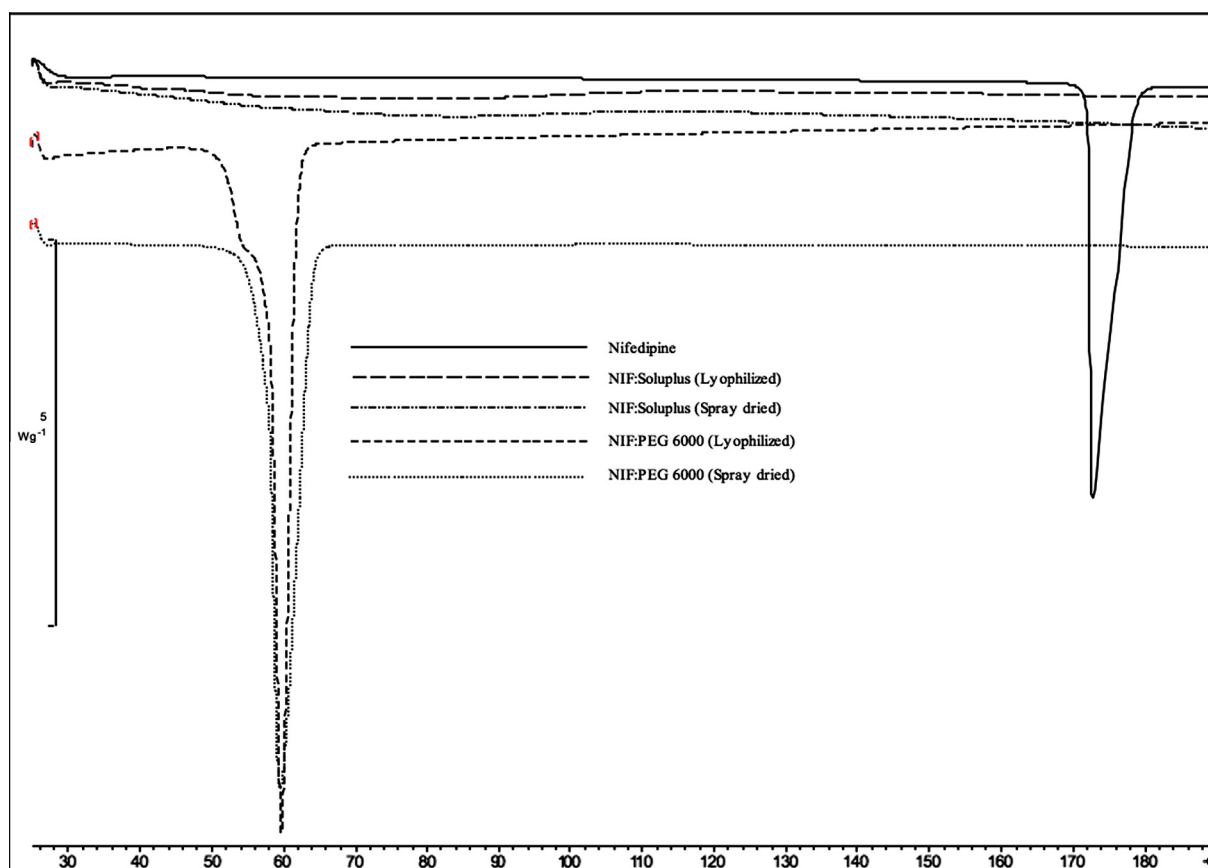


**Figure 7b** DSC thermograms for NIF mixtures with Soluplus® and with PEG 6000 at a mass ratio of 1:9 stored for six months at 0% RH and 25 °C.

NIF have melting endotherms around 170 °C; however, the thermodynamic driving force for solubility in Soluplus® is larger for SMX than for NIF (Altamimi and Neau, 2016). Therefore, it was expected that Soluplus® would dissolve SMX to a larger extent than NIF when making a solid dispersion.

Thermograms for the spray dried mixtures of NIF-PEG 6000 at 1:5 and 1:9 mass ratios reveal the absence of the NIF melting endotherm, indicating a complete conversion of crystalline NIF to its amorphous form or complete molecular level dispersion of the drug in the polymer matrix, see Fig. 4b.

#### 4.1.2. Lyophilized solid dispersions

Thermograms for the lyophilized SMX-Soluplus® and SMX-PEG 6000 mixtures are found in Figs. 5a and 5b, respectively. The melting endotherm was obvious in the thermogram for each dispersion with the 1:1 mass ratio, indicating the presence of crystalline drug. The melting endotherm is not evident in the thermograms for mixtures with higher polymer levels.

In Figs. 6a and 6b, the melting endotherm was absent except for 1:1 ratio. In particular, Fig. 6a, a recrystallization peak was found before the melting of nifedipine.

The preparation methods for the solid dispersion mixtures are of crucial importance. The detectable sharp melting endotherm for the lyophilized 1:1 mixture of NIF or SMX with PEG 6000 proves the superiority of spray drying to form solid dispersions. The freezing step in lyophilization fixes the solution components in space because the viscosity of the

liquid would rise quickly, whereas spray drying should allow a greater time frame over which rearrangement of solute molecules can take place as the solvent evaporates from each sprayed drop. In the freezing step, bound water does not freeze. This bound water will not sublime in the reduced pressure environment (Abdelwahed et al., 2006), but is more likely to be removed during secondary drying in a lyophilizer or with sufficient extended time in the desiccator at room temperature. In spray drying, bound water should evaporate due to the higher temperature providing sufficient energy to break the bonds of water with the polymer hydrophilic functional group(s) that lead to bound water.

Water in the lyophilized mixture is more likely found in the amorphous part of the drug but its presence can induce crystallization. Such induction occurs due the greater mobility that the water gives to the amorphous form of the drug (Vlassios Andronis and George, 1996; Grisedale et al., 2012). For every SMX:Soluplus® ratio, single detectable  $T_g$  was missing in lyophilized mixtures, which also indicates less efficient mixing of the two in the lyophilized mixtures.

When SMX- or NIF-PEG 6000 samples were lyophilized, the solid dispersion successfully maintained the amorphous form of the drug at higher polymer levels in the samples, with mass ratios of 1:5, and 1:9 (Figs. 5b and 6b, respectively). At the 1:1 mass ratio, the melting endotherms for each drug were detected, exhibiting a trend similar to that observed with Soluplus®. It is important to note that, polyethylene glycol,

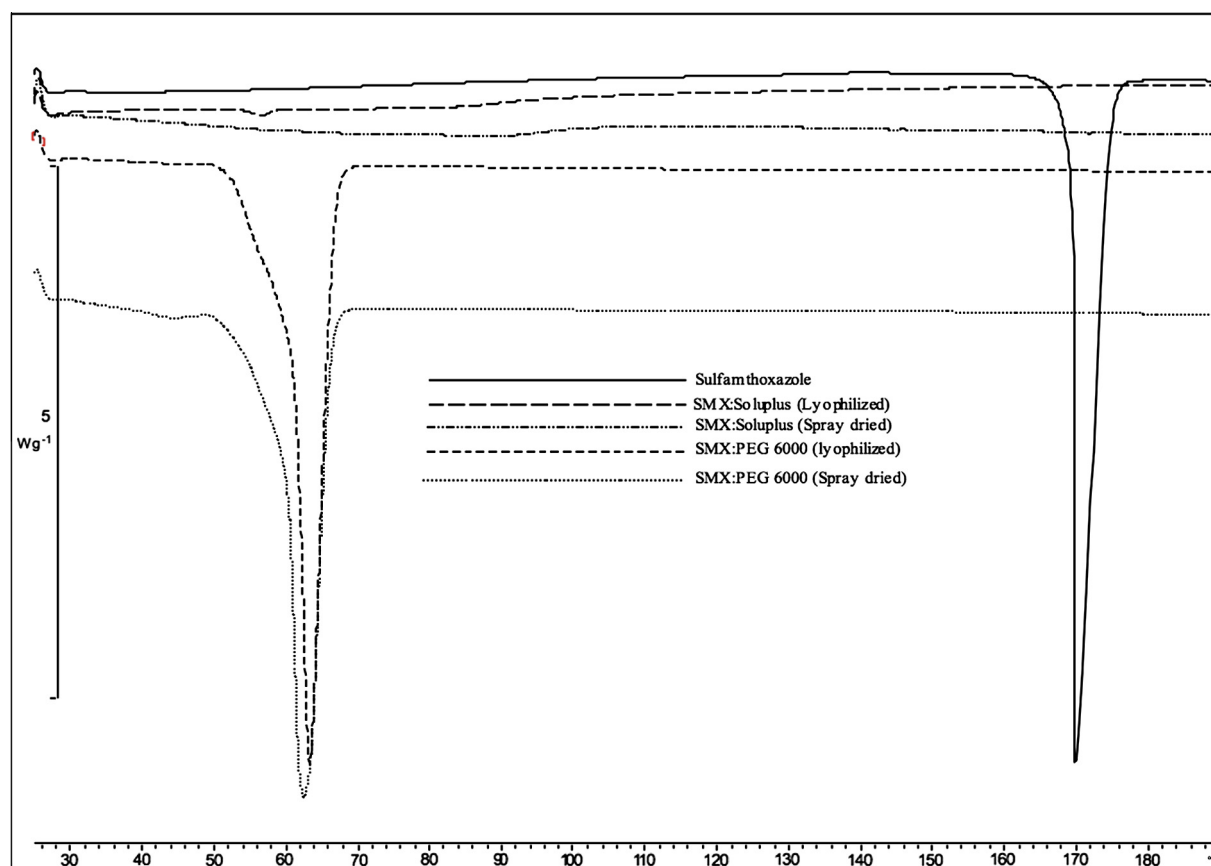


**Figure 7c** DSC thermograms for SMX mixtures with Soluplus<sup>®</sup> and with PEG 6000 at a mass ratio of 1:9 stored for six months at 0% R.H. and 50 °C.

at different molecular weights, has been used to form eutectic mixtures (Vippagunta et al., 2007). In their study, they have found mixing PEG with a crystal drug at ratios around the eutectic point showed similar improvement in the dissolution rate. Furthermore, Law et al., presented unchanged PXRD patterns for PEG:fenofibrate at or around the eutectic point (Law et al., 2003). Therefore, we expect an improvement in the dissolution rate at the selected ratios whether or not we formed an eutectic mixture (will be discussed later in this paper).

#### 4.2. Drug stability studies

The drug and the 1:9 mass ratio drug:polymer mixtures, prepared using either spray drying or lyophilization techniques, are subjected to a 6 month study under different temperature conditions. No recrystallization was found with either of the dispersed drugs (see Figs. 7a–7d).

#### 4.3. Fourier transform infrared spectroscopy

The energy in the infrared IR region is not sufficient to excite electrons of a molecule. Upon absorption, however, the energy is enough to stretch or bend the bonds of a particular molecule. Therefore, the vibrational frequencies of certain chemical bonds involving specific atoms are detected using IR spec-

troscopy (Watson, 2005). The IR spectrum provides the fingerprint of different chemical substances and specifically can detect the presence of newly formed bonds when the molecules are dispersed in polymers (Huang et al., 2008).

The IR spectrum for crystalline SMX is found in Fig. 8a. For SMX, the first three distinctive peaks starting from the higher wave numbers are attributed to N–H vibrations. NH<sub>2</sub> stretching shows sharp peaks at 3468 and 3378 cm<sup>-1</sup> for asymmetric and symmetric stretching, respectively. The detected peak at 3299 cm<sup>-1</sup> is attributed to N–H stretching in the amide functional group. C–H stretching shows a clear peak at 3144 cm<sup>-1</sup> (Takasuka and Nakai, 2001). C–C and C–N vibrational stretching is assigned to the peaks at 1597 and 1502 cm<sup>-1</sup>, respectively. The peaks at 1267, 1092, and 1043 cm<sup>-1</sup> are attributed to the SO<sub>2</sub> stretching vibrations (Vijaya Chamundeeswari et al., 2014).

The crystalline NIF IR spectrum is found in Fig. 8a. The distinctive vibrational bands at 3332, and 1682–1690 cm<sup>-1</sup> are attributed to N–H and C=O, respectively (Huang et al., 2008). The peak at 2954 cm<sup>-1</sup> is assigned to C–H aliphatic stretching. NO<sub>2</sub> symmetric stretching is found at 1350 cm<sup>-1</sup> (Chan et al., 2004).

Soluplus<sup>®</sup> showed a broad peak centered at 3463 cm<sup>-1</sup> that is attributed to O–H vibrational stretching. C–H stretching is found to be the peak at 2933 cm<sup>-1</sup>. Peaks at 1739, and 1635 cm<sup>-1</sup> are attributed to C=O in the ester and tertiary amide, respectively (Homayouni et al., 2014). The ether

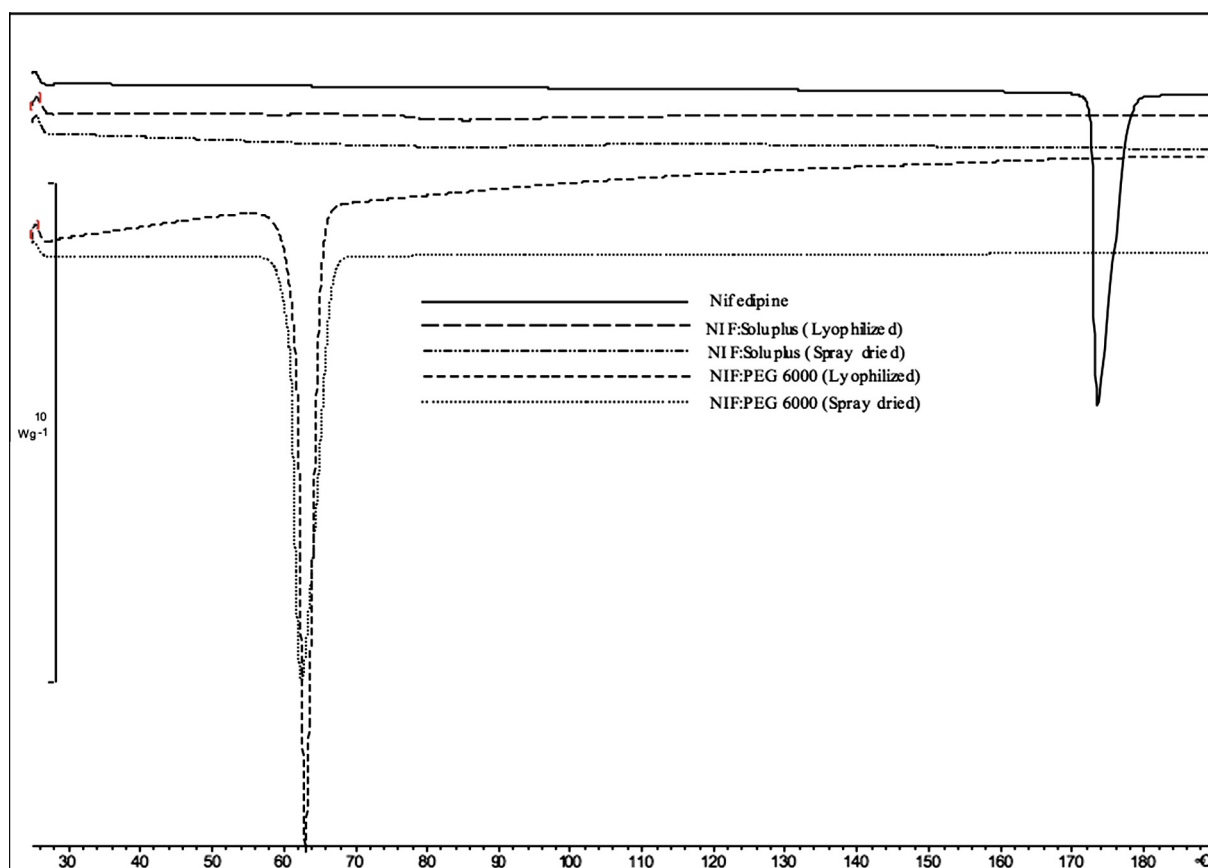


**Figure 7d** DSC thermograms for NIF mixtures with Soluplus® and with PEG 6000 at a mass ratio of 1:9 stored for six months at 0% RH and 50 °C.

C—O—C has a distinctive peak at  $1483\text{ cm}^{-1}$  (Shamma and Basha, 2013).

PEG 6000 showed peaks at  $3439$ ,  $2887$ , and  $1113\text{ cm}^{-1}$  that are attributed to O—H, C—H and C—O—C vibrational stretching (Vijaya Kumar and Mishra, 2006; Ruan et al., 2005; Sawhney et al., 1993; Van den Mooter et al., 1998). The observed peak wave numbers in the IR spectra of each functional group are summarized in Table 2, along with the wave number found in the literature.

There are different functional groups in SMX and NIF that are capable of donating or accepting protons to form hydrogen bonds. The primary amine and the nitrogen in the sulfonamide group in SMX can donate protons to higher electronegativity atoms. In fact, SMX is expected to form hydrogen bonding with itself when the two oxygen atoms associated with the sulfur atom ( $\text{SO}_2$ ) accept the protons. Also, the nitrogen atom in the isoxazole ring can also act as a proton acceptor.

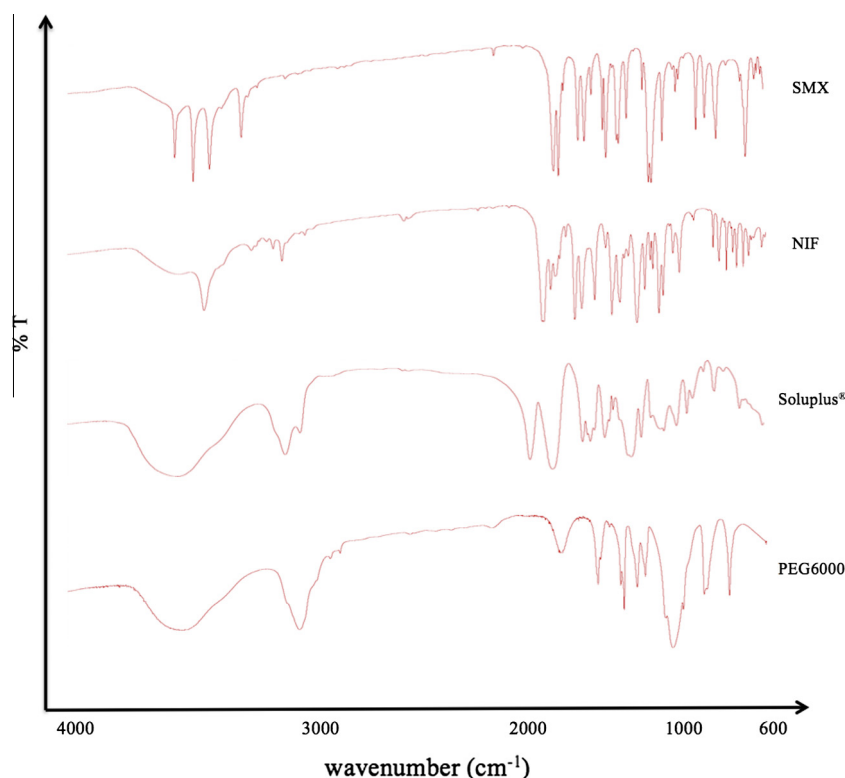
The proton donor site in NIF is the nitrogen in the dihydropyridine ring. The oxygens in the carbonyl functional groups are proton acceptors. The  $\text{NO}_2$  functional group is expected to have no hydrogen bonding capability (Huang et al., 2008). Soluplus® has carbonyl, hydroxyl, and ether functional groups capable of hydrogen bonding. PEG 6000 likewise can donate or accept a proton through the hydroxyl groups and the oxygen in each of the ether groups.

Fig. 8b shows the IR spectrum of spray dried (S) and lyophilized (L) SMX with either Soluplus® or PEG 6000. For

the SMX-Soluplus® solid dispersion, the four distinctive peaks between  $3000$  and  $3500\text{ cm}^{-1}$  for crystalline SMX have disappeared. This disappearance is ascribed to the disruption of hydrogen bonding between the SMX molecules and forming new bonds with the polymer. The shift in the broad peak from  $3463\text{ cm}^{-1}$  for neat Soluplus® to  $3448$  and  $3455\text{ cm}^{-1}$  for the spray dried and lyophilized SMX-Soluplus® mixtures is postulated to be the O—H stretching vibrations which strongly indicate hydrogen bond formation with either the primary amine or one of the oxygen atoms found on the sulfur. There is a small but detectable shoulder at  $3230\text{ cm}^{-1}$ , which might indicate a stretch of the amide N—H in SMX. The two carbonyl peaks at  $1739$ , and  $1635\text{ cm}^{-1}$  have shifted to lower wave numbers in the mixture. The new peaks are evident at  $1736$ ,  $1625$ , and  $1621\text{ cm}^{-1}$ , suggesting a new hydrogen bond stretching with the primary amine and amide N—H.

The broad peak at  $3439\text{ cm}^{-1}$  for neat PEG 6000 has shifted to  $3443\text{ cm}^{-1}$  for spray dried and lyophilized dispersed mixtures. Such a shift is postulated to be stretching in the hydrogen bond of the hydroxyl groups of the polymer. The ether group shifted to  $1112\text{ cm}^{-1}$  for the dispersed mixtures. This slight difference might not be compelling for hydrogen bond formation; however, the difficulty to demonstrate the hydrogen bond formation with PEG 6000 has been reported elsewhere (Van den Mooter et al., 1998).

Fig. 8c shows the IR spectrum of spray dried (S) and lyophilized (L) NIF with either Soluplus® or PEG 6000. For



**Figure 8a** FTIR analysis for the used materials.

NIF-Soluplus® solid dispersion, the broad peak for Soluplus® has shifted to  $3459\text{ cm}^{-1}$ . The shift in this peak is attributed to hydrogen bond formation between the carbonyl group found in NIF with the hydroxyl group found in Soluplus®. The small shoulder at  $3285$  is postulated to be N—H stretching of NIF due to hydrogen bond formation with Soluplus® carbonyl or ether groups. The carbonyl groups of NIF exhibit sharp peaks at  $1682\text{--}1690\text{ cm}^{-1}$ , whereas Soluplus® exhibits distinctive carbonyl peaks at  $1739$  and  $1635\text{ cm}^{-1}$ . For the dispersions, however, the peak moved higher to  $1701\text{ cm}^{-1}$  which is attributed to the stretch in the C=O when engaged in hydrogen bond formation with the polymer. Huang et al., suggested that the peak at  $1701\text{ cm}^{-1}$  indicates formation of amorphous NIF, and the carbonyl stretch for NIF at  $1702\text{--}1728\text{ cm}^{-1}$  should indicate hydrogen bond formation (Huang et al., 2008). However, forming an amorphous drug is expected and it was previously confirmed using DSC analysis. In addition, having carbonyl groups in both the polymer and the drug might obscure the shift of the stretch in the NIF carbonyl groups. Soluplus® carbonyl group peaks have shifted to  $1736$ ,  $1636$  and  $1739$ ,  $1632$  for spray dried and lyophilized mixtures, respectively.

The change in the wave number of the PEG 6000 broad peak from  $3439$  to  $3443\text{ cm}^{-1}$  in NIF-PEG 6000 dispersions is similar to the one found for SMX-PEG 6000 dispersions, which is due to stretching in the hydroxyl groups of the polymer. The small shoulder at  $3327\text{ cm}^{-1}$  is expected to be the vibrational stretch of N—H upon hydrogen bond formation with the polymer. The carbonyl group exhibits distinctive peaks at  $1682\text{--}1690\text{ cm}^{-1}$ . The absence of any stretching indicates that there was no hydrogen bond between the carbonyl group and the polymer.

The FTIR studies exhibit compelling evidences of change in the vibrational stretching within the different dispersions. The missing distinctive peaks, for instance, between pure SMX and SMX in dispersions are attributed to the inclusion of the drug in the polymer cavity (Guyot et al., 1995). Using the drug in smaller mass ratios with the polymer might prevent the instrument from acknowledging the vibrational stretching.

Between spray drying and lyophilization there were no significant differences in the IR spectra. The lack of any differences indicates that the preparation methods used to form solid dispersion have comparable efficiency.

#### 4.4. Drug dissolution studies

It is crucial to test the dissolution characteristics of the drug and the drug-polymer mixtures prepared using different methods. As described in the method section, the preparation parameters were kept exactly the same, except when final products were made. Therefore, we expect any differences to be due to the preparation methods only. Two different enzyme-free media were selected, namely simulated intestinal fluid SIF ( $\text{pH} = 6.8 \pm 0.1$ ) and simulated gastric fluid SGF ( $\text{pH} = 1.2 \pm 0.1$ ) at  $37 \pm 0.2\text{ }^{\circ}\text{C}$ . The model drugs, only, were tested in water for comparison. Each drug is ionized at a particular pH range or ranges. Sulfamethoxazole has two pKa values, namely  $1.7$  and  $5.7$ . At pH above  $5.7$  SMX becomes anionic losing the proton on  $-\text{SO}_2-\text{NH}-$  group. In very acidic conditions, with pH less than  $1.7$ , the cationic form of SMX is found by protonating the aromatic  $\text{NH}_2$  group. For pH between  $1.7$  and  $5.7$  SMX is expected to be uncharged (Gokturk et al., 2012; Lucida et al., 2000). For NIF, however,

**Table 2** The characteristic vibrational stretching wave numbers for functional groups found in the materials and their corresponding values from the literature.

Assignments	Literature SMX wave numbers (cm <sup>-1</sup> )	Experimental SMX wave numbers (cm <sup>-1</sup> )	Literature NIF wave numbers (cm <sup>-1</sup> )	Experimental NIF wave numbers (cm <sup>-1</sup> )	Literature Soluplus® wave numbers (cm <sup>-1</sup> )	Experimental Soluplus® wave numbers (cm <sup>-1</sup> )	Literature PEG 6000 wave numbers (cm <sup>-1</sup> )	Experimental PEG 6000 wave numbers (cm <sup>-1</sup> )
as,1(N—H)	3470 <sup>a</sup> , 3467 <sup>b</sup>	3468	—	—	—	—	—	—
s,1(N—H)	3381 <sup>a</sup> , 3378 <sup>b</sup>	3378	—	—	—	—	—	—
2(N—H)	3301 <sup>b</sup>	3299	3332 <sup>c</sup> , 3330 <sup>d</sup>	3332	—	—	—	—
O—H	—	—	—	—	3449 <sup>e</sup>	3463	3445 <sup>g</sup> , 3446 <sup>h</sup> , 3510 <sup>k</sup>	3439
C—H	3145 <sup>a</sup> , 3143 <sup>b</sup>	3144	2953 <sup>d</sup>	2954	2928 <sup>e</sup>	2933	2887 <sup>g</sup> , 2889 <sup>h</sup> , 2880 <sup>k</sup>	2887
C—C	1619 <sup>b</sup> , 1597 <sup>b</sup>	1621, 1597	—	—	—	—	—	—
C=O	—	—	(1679, 1689) <sup>e</sup> (1679, 1682) <sup>d</sup>	(1682, 1690)	(1739, 1643) <sup>e</sup> (1736, 1635) <sup>f</sup>	(1739, 1635)	—	—
C—O—C	—	—	—	—	1477 <sup>e</sup>	1483	1110 <sup>g,l</sup>	1113
N=O	—	—	1530 <sup>d</sup>	1530	—	—	—	—
S=O	1266 <sup>b</sup> , 1091 <sup>b</sup>	1267, 1092	—	—	—	—	—	—

(a, as) are asymmetric and symmetric vibrational stretching.

(1, 2) are primary and secondary amines.

<sup>a</sup> Reference Takasuka and Nakai (2001).

<sup>b</sup> Reference Vijaya Chamundeeswari et al. (2014).

<sup>c</sup> Reference Huang et al. (2008).

<sup>d</sup> Reference Chan et al. (2004).

<sup>e</sup> Reference Homayouni et al. (2014).

<sup>f</sup> Reference Shamma and Basha (2013).

<sup>g</sup> Reference Vijaya Kumar and Mishra (2006).

<sup>h</sup> Reference Ruan et al. (2005).

<sup>k</sup> Reference Sawhney et al. (1993).

<sup>l</sup> Reference Van den Mooter et al. (1998).

the pKa was reported to be around 1 (Zhang et al., 1997; Zendelovska et al., 2006). Therefore, except in very acidic condition of pH ≤ 1.0, NIF is expected to be predominantly uncharged.

A three hour dissolution study proved to be sufficient to identify the highest drug concentration (Konno et al., 2008). Reduction in the drug concentration due to recrystallization can, therefore, be identified (Tanno et al., 2004).

In Fig. 9a, pure SMX exhibited a high dissolution rate in water and SIF. Spray dried SMX with PEG 6000 revealed the higher dissolution rate with nearly complete drug dissolution in the first 15 min of the dissolution profile. The concentration was maintained at 91% at 180 min, which suggests a slight precipitation of SMX under these conditions. SMX-Soluplus® spray dried mixture exhibits a slower release rate than does the pure SMX. Soluplus® is an amphiphilic polymer that might contribute to the dissolution with a slower rate due to its own slower dissolution rate. The drug release profile for Soluplus®, however, provided 85% release at 180 min. It is important to note that SMX-Soluplus® spray dried mixture showed a potential of continual increase in SMX concentration after 3 h period.

In Fig. 9b, the dissolution rate and the percentage release of pure SMX in SGF are lower than the one found in SIF. It suggests that the cationic form of SMX has a lower dissolution rate and overall solubility than the anionic form. PEG 6000 was effective in enhancing the drug release rate and in maintaining the drug concentration over the experimental time period. SMX-Soluplus® spray dried mixture provided a complete dissolution of the drug after 150 min in SGF.

In Fig. 9c, SMX and the lyophilized mixtures exhibited high, but similar, dissolution rates. The lyophilized product showed an enhanced dissolution rate for SMX-Soluplus® mixture with similar tendency for greater improvement in the drug concentration with time. A similar trend was observed for SMX-PEG 6000 with a slight reduction in drug concentration after 120 min, which might be attributed to precipitation.

In Fig. 9d, the dissolution rate for lyophilized SMX-PEG 6000 in SGF is slower than in SIF, whereas the SMX-Soluplus® mixture maintained a complete dissolution level for the last 90 min. The two polymers maintain higher drug concentrations than the pure drug can achieve.

The spray dried mixtures are more sensitive to the ionization form of SMX. It has been reported that at high Soluplus®



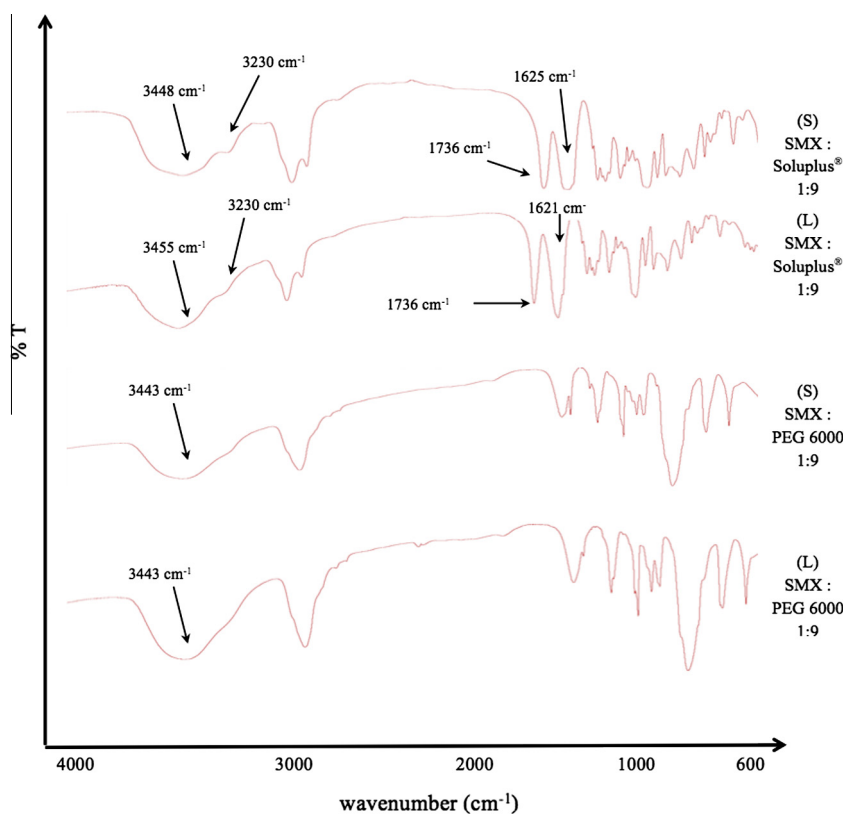


**Figure 8b** FTIR analysis for SMX-polymer mixtures (S denotes spray dried, and L denotes lyophilized).

concentrations the drug should exhibit slower dissolution rate due to the increase in the medium viscosity (Homayouni et al., 2014). Furthermore, Soluplus® forms micelles (Yu et al., 2013) and it was suggested that polymers that form micelles with higher loading and lower polymer concentration in the medium should induce less interaction between the drug and the polymer and, thus, impose greater pressure on the micelle wall. Therefore, they enhance the dissolution rate (Yu et al., 2013; Huh et al., 2005), but might exceed the capacity of the micelles to contain the poorly soluble drug. In contrast, when the PEG 6000 ratio increased, a large increase in drug dissolution rate and overall drug concentration were found. However, an optimal PEG 6000: drug ratio is likely to exist (Guyot et al., 1995; Ruan et al., 2005; Save and Venkitachalam, 1992) above which PEG can no longer improve on this function. We hypothesize that the enhanced dissolution performance by the lyophilized mixtures is attributed to the higher porosity that led to improve wettability of the materials. Such improvement, also, obscured the ionization effect of the drug. PEG 6000 and Soluplus® maintained higher drug concentration indicating a potential to maintain a supersaturated state of drug in the medium. No significant reduction in the drug concentration was observed over the experimental time frame. SMX inherently has a fast dissolution rate at these media pH which might negate the advantages to solid dispersions using these polymers.

In Fig. 10a, pure NIF exhibited a low dissolution rate in SIF showing only 19% drug dissolved after three hours. In water, however, NIF has an improved dissolution rate and

exhibited 35% drug dissolved at 180 min. Spray dried NIF with PEG 6000 provided a higher dissolution rate with incomplete drug dissolution at 3 h. Such incomplete dissolution has been reported elsewhere (Hecq et al., 2005). The sample allowed more than 40% to be released rapidly in the first few minutes and then slowly achieved 56% released at 180 min. Soluplus® again contributed to a slower dissolution rate. The drug release profile for Soluplus®, however, provided 49% drug release at 180 min, but showed a burst release of 20% drug released in a few minutes.

NIF has a pKa of about 1 and is expected to be mostly ionized at a pH of 1.2. In Fig. 10b, the dissolution rate and the percentage dissolved at any time for pure NIF in SGF are higher than found in SIF. This simply confirms that the ionized form of NIF has a higher solubility than its unionized form. Spray dried NIF with PEG 6000 provided a higher dissolution rate with incomplete drug dissolution at 3 h in each medium. The concentration rapidly achieved greater than 60% in the first few minutes and slowly increased to reach 86% at 180 min. The drug release profile for NIF dispersion in Soluplus®, however, provided 95% release at 180 min in SGF, but showed a lower level of drug release in the first few minutes than provided by PEG 6000. It is important to note that the performance of the spray dried mixtures in the different media displayed the potential for continued release of NIF after 180 min.

In Fig. 10c, a rapid dissolution rate was found for the lyophilized NIF dispersion in PEG 6000. However, a slight reduction in NIF concentration after the first reading might indicate

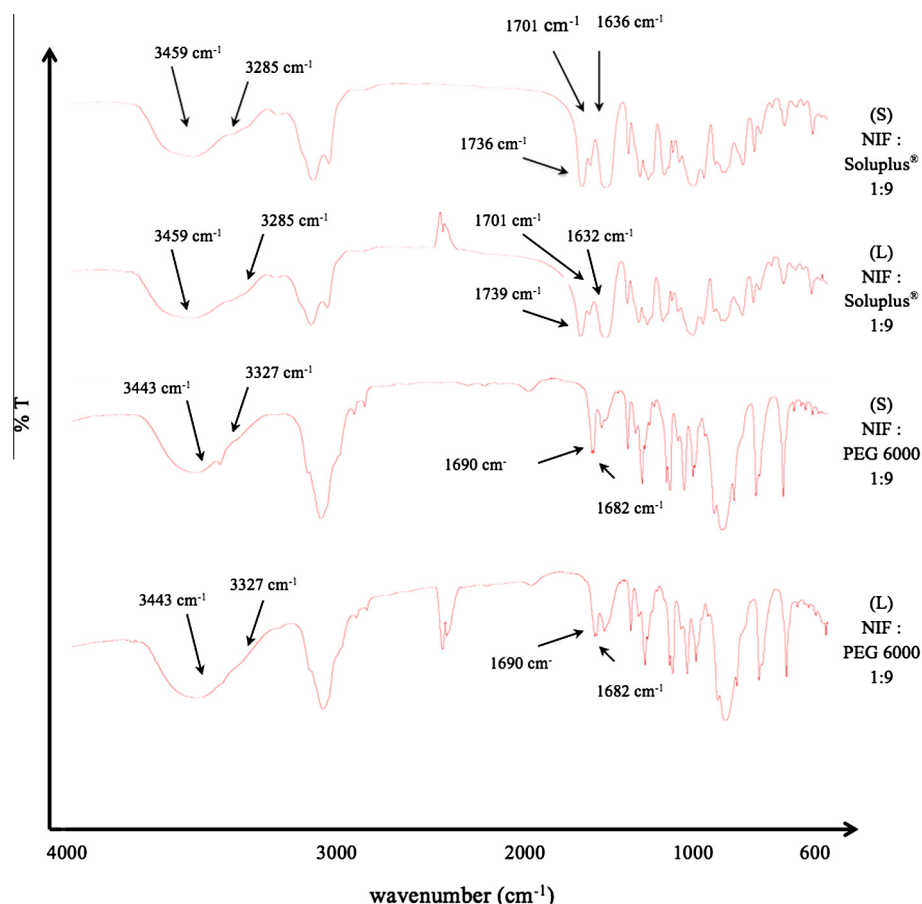


**Figure 8c** FTIR analysis for NIF-polymer mixtures (S denotes spray dried, and L denotes lyophilized).

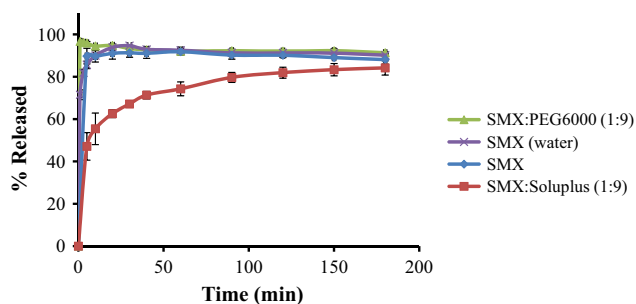


**Figure 9a** Sulfamethoxazole and spray dried SMX with Soluplus® or PEG 6000 in SIF ( $n = 3$ ). SMX alone in deionized water was added for comparison. Error bars represent standard deviation.

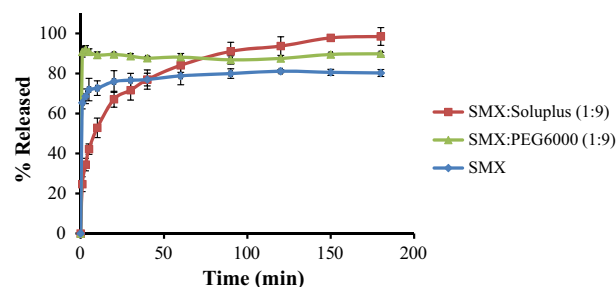


**Figure 9b** Sulfamethoxazole and spray dried SMX with Soluplus® or PEG 6000 in SGF ( $n = 3$ ). Error bars represent standard deviation.

precipitation of a portion of the released drug. The lyophilized product showed an enhanced dissolution rate and extent of drug released in comparison with the performance of the spray dried mixtures. A similar trend was observed for NIF dispersions in Soluplus® with a slower release rate followed by an improved drug release at 180 min.

In Fig. 10d, the dissolution rate and the extent of drug released for lyophilized NIF-PEG 6000 in SGF are higher than found in SIF. An enhanced dissolution rate and complete dissolution for NIF-Soluplus® were observed.

Soluplus® and PEG 6000 demonstrated tremendous potential for enhancing the dissolution rate and maintaining the supersaturated state for the model drugs. That can be attributed to different reasons. The first reason is the ability of the polymers to inhibit the crystallization tendency of the amorphous materials in supersaturated states (Tanno et al., 2004). Secondly, polymer behavior in the medium can enhance the equilibrium concentration of the drug (Konno et al., 2008; Loftsson et al., 1996), PEG by acting as a cosolvent and Soluplus® by micelle formation. Furthermore, others suggested

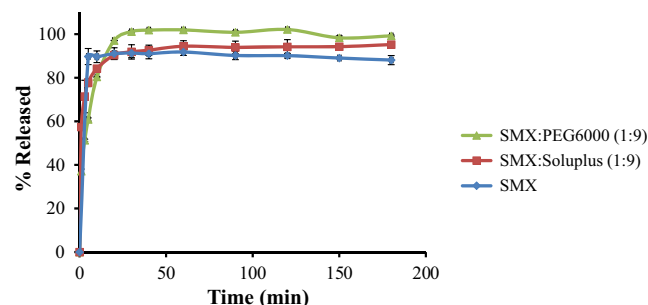


**Figure 9c** Sulfamethoxazole and lyophilized SMX with Soluplus® or PEG 6000 in SIF ( $n = 3$ ). Error bars represent standard deviation.

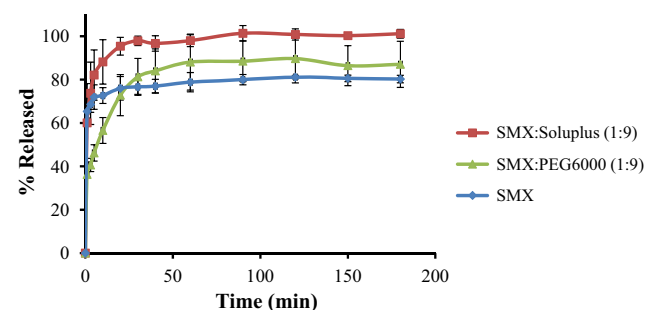


**Figure 9d** Sulfamethoxazole and lyophilized SMX with Soluplus® or PEG 6000 in SGF ( $n = 3$ ). Error bars represent standard deviation.

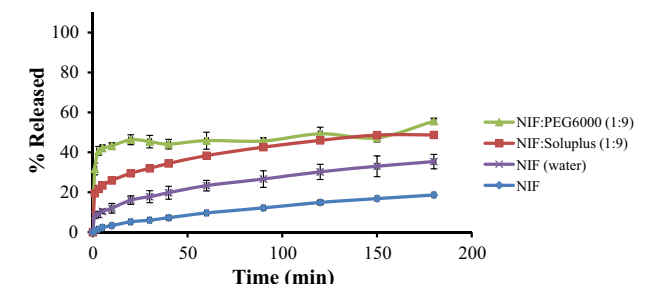


**Figure 10a** Nifedipine and spray dried NIF with Soluplus® or PEG 6000 in SIF ( $n = 3$ ). NIF alone in deionized water was added for comparison. Error bars represent standard deviation.

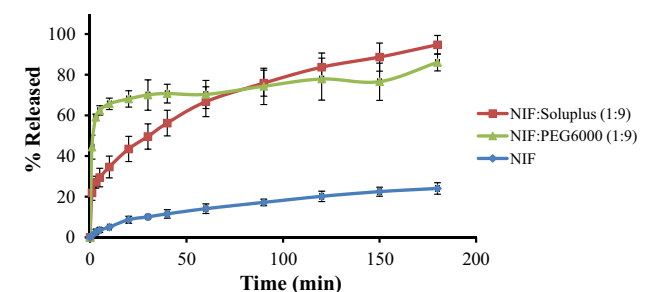


**Figure 10b** Nifedipine and spray dried NIF with Soluplus® or PEG 6000 in SGF ( $n = 3$ ). Error bars represent standard deviation.

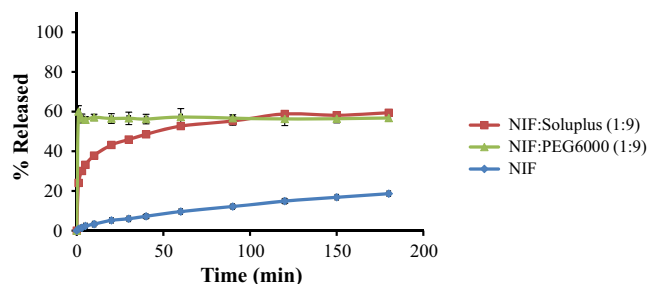


**Figure 10c** Nifedipine and lyophilized NIF with Soluplus® or PEG 6000 in SIF ( $n = 3$ ). Error bars represent standard deviation.

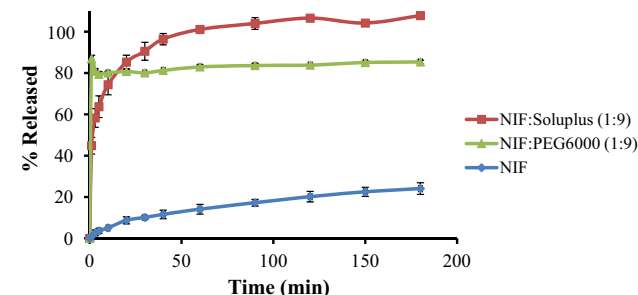


**Figure 10d** Nifedipine and lyophilized NIF with Soluplus® or PEG 6000 in SGF ( $n = 3$ ). Error bars represent standard deviation.

that dispersed mixtures enhanced dissolution rates by improved wetting of drug due to the inherent higher dissolution rate of hydrophilic polymers (Fouad et al., 2011; Khan et al., 2012).

Both Soluplus® and PEG 6000 showed an initial burst release of drug, which is expected from highly soluble polymers (Khan et al., 2012; Nagy et al., 2012; Karavas et al., 2007). However, PEG 6000-drug mixtures exhibited a slight reduction in concentration which might be attributed to precipitation. As an amphiphilic polymer, Soluplus® provided a slower dissolution rate for SMX and NIF dispersions at this particular mass ratio, yet this was followed by a higher extent of drug released than observed with PEG 6000 dispersions. The ionization state of the drug will also enhance or reduce the dissolution rate and limit the equilibrium drug concentration based on its inherent characteristics. This phenomenon is demonstrated well when using NIF as a model drug. The lyophilized mixtures showed higher dissolution rates and extents of drug release than each spray dried counterpart.

#### 4.5. Mathematical models for the release profiles

The kinetic models for the release profiles for different mixtures are found in Tables 3 and 4. Release profiles for spray dried SMX dispersions with Soluplus® in simulated intestinal and gastric fluids are best described by the Ritger-Peppas equation. This equation utilizes  $n$  as the exponent to describe the release mechanism. The diffusion coefficient  $n$  indicates a Fickian diffusion at a value of 0.45 and case II transport at a value  $> 0.89$ . An anomalous release mechanism is expected when  $0.45 < n < 0.89$  (Khan et al., 2012; Shoaib et al., 2006). However,  $n$  with values less than 0.45 have been

**Table 3** The kinetic models for dissolution of SMX or release of SMX from Soluplus® or PEG 6000 dispersions prepared using spray drying or lyophilization techniques.  $\pm$  standard errors ( $p < 0.05$ ).

Materials	Zero Order		First Order		Higuchi		Hixson-Crowell		Ritger-Peppas		
	$R^2$	$K_0$ (min <sup>-1</sup> )	$R^2$	$K_1$ (min <sup>-1</sup> )	$R^2$	$K_H$ (min <sup>-1/2</sup> )	$R^2$	$K_{HC}$ (min <sup>-1/3</sup> )	$R^2$	$n$	$K_{RP}$ (min <sup>-n</sup> )
<i>Spray Dried Materials</i>											
SMX:PEG 6000 (1:9) (SIF)	—	—	—	—	—	—	—	—	—	—	—
SMX (Water)	—	—	—	—	—	—	—	—	—	—	—
SMX (SIF)	—	—	—	—	—	—	—	—	—	—	—
SMX:Soluplus® (1:9) (SIF)	0.937	0.0065 $\pm 0.001$	0.9725	0.0167 $\pm 0.0016$	0.9829	0.0573 $\pm 0.0044$	0.9146	0.0110 $\pm 0.0013$	0.9996	0.1929 $\pm 0.0059$	0.3502 $\pm 0.0064$
SMX:PEG 6000 (1:9) (SGF)	—	—	—	—	—	—	—	—	—	—	—
SMX (SGF)	0.8185	0.0049 $\pm 0.0013$	0.8577	0.0171 $\pm 0.004$	0.9224	0.0291 $\pm 0.0049$	0.8451	0.0101 $\pm 0.0025$	0.9712	0.0497 $\pm 0.005$	0.654 $\pm 0.0064$
SMX:Soluplus® (1:9) (SGF)	0.9389	0.021 $\pm 0.0031$	0.9843	0.0422 $\pm 0.0031$	0.9958	0.122 $\pm 0.0046$	0.9725	0.0301 $\pm 0.0029$	0.9992	0.3399 $\pm 0.006$	0.2421 $\pm 0.0034$
<i>Lyophilized Materials</i>											
SMX:PEG 6000 (1:9) (SIF)	0.9877	0.0594 $\pm 0.0066$	0.9981	0.1187 $\pm 0.0052$	0.9999	0.1924 $\pm 0.0009$	0.9956	0.0851 $\pm 0.0057$	0.9988	0.308 $\pm 0.012$	0.3689 $\pm 0.0056$
SMX:Soluplus® (1:9) (SIF)	—	—	—	—	—	—	—	—	—	—	—
SMX:PEG 6000 (1:9) (SGF)	0.9913	0.0191 $\pm 0.001$	0.9992	0.0452 $\pm 0.0007$	0.9875	0.1079 $\pm 0.007$	0.9995	0.0305 $\pm 0.0004$	0.9527	0.262 $\pm 0.035$	0.320 $\pm 0.026$
SMX:Soluplus® (1:9) (SGF)	—	—	—	—	—	—	—	—	—	—	—

**Table 4** The kinetic models for dissolution of SMX or release of SMX from Soluplus® or PEG 6000 dispersions prepared using spray drying or lyophilization techniques.  $\pm$  standard errors ( $p < 0.05$ ).

Materials	Zero Order		First Order		Higuchi		Hixson-Crowell		Ritger-Peppas		
	$R^2$	$K_0$ (min <sup>-1</sup> )	$R^2$	$K_1$ (min <sup>-1</sup> )	$R^2$	$K_H$ (min <sup>-1/2</sup> )	$R^2$	$K_{HC}$ (min <sup>-1/3</sup> )	$R^2$	$n$	$K_{RP}$ (min <sup>-n</sup> )
<i>Spray Dried Materials</i>											
NIF:PEG 6000 (1:9) (SIF)	0.6102	0.0007 $\pm 0.0002$	0.6510	0.0013 $\pm 0.0003$	0.6890	0.0110 $\pm 0.0023$	0.6385	0.0009 $\pm 0.0002$	0.7716	0.0677 $\pm 0.0122$	0.358 $\pm 0.017$
NIF (Water)	0.9437	0.0015 $\pm 0.0001$	0.9632	0.0019 $\pm 0.001$	0.9984	0.0224 $\pm 0.0003$	0.9571	0.0015 $\pm 0.0001$	0.9891	0.344 $\pm 0.014$	0.0579 $\pm 0.0037$
NIF (SIF)	0.9720	0.0010 $\pm 0.0001$	0.9798	0.0011 $\pm 0.0001$	0.9948	0.0145 $\pm 0.0003$	0.9773	0.0009 $\pm 0.0000$	0.9990	0.6084 $\pm 0.0091$	.0080 $\pm 0.0003$
NIF:Soluplus® (1:9) (SIF)	0.9018	0.0016 $\pm 0.0002$	0.9318	0.0026 $\pm 0.0002$	0.9903	0.0248 $\pm 0.0008$	0.9225	0.0018 $\pm 0.0002$	0.9833	0.2075 $\pm 0.0097$	0.1663 $\pm 0.0068$
NIF:PEG 6000 (1:9) (SGF)	0.5809	0.0063 $\pm 0.0027$	0.6661	0.0160 $\pm 0.0057$	0.7372	0.0468 $\pm 0.0140$	0.6375	0.0096 $\pm 0.0036^a$	0.9679	0.213 $\pm 0.041$	0.452 $\pm 0.023$
NIF (SGF)	0.9316	0.0012 $\pm 0.0001$	0.9485	0.0014 $\pm 0.0001$	0.9978	0.0187 $\pm 0.0003$	0.9431	0.0011 $\pm 0.0001$	0.9970	0.511 $\pm 0.013$	0.0173 $\pm 0.0010$
NIF:Soluplus® (1:9) (SGF)	0.9721	0.0074 $\pm 0.0005$	0.9962	0.0139 $\pm 0.0004$	0.9971	0.0654 $\pm 0.0014$	0.9914	0.0092 $\pm 0.0003$	0.9811	0.2761 $\pm 0.0019$	0.195 $\pm 0.011$
<i>Lyophilized Materials</i>											
NIF:PEG 6000 (1:9) (SIF)	—	—	—	—	—	—	—	—	—	—	—
NIF:Soluplus® (1:9) (SIF)	0.7526	0.0017 $\pm 0.0003$	0.8138	0.0032 $\pm 0.0005$	0.9158	0.0271 $\pm 0.0026$	0.7943	0.0021 $\pm 0.0003$	0.9901	0.1695 $\pm 0.0060$	0.2553 $\pm 0.0064$
NIF:PEG 6000 (1:9) (SGF)	—	—	—	—	—	—	—	—	—	—	—
NIF:Soluplus® (1:9) (SGF)	0.9163	0.0304 $\pm 0.0065$	0.9719	0.0812 $\pm 0.0098$	0.9818	0.134 $\pm 0.028$	0.9567	0.0479 $\pm 0.0072$	0.9944	0.218 $\pm 0.017^a$	0.4521 $\pm 0.0097$

<sup>a</sup> For ( $p > 0.05$ ).

**Table 5** The release profile comparisons for SMX-polymer mixtures.

Reference material	SMX(SIF)		SMX(SGF)		SMX: Soluplus® (1:9) (SIF)	SMX: PEG6000 (1:9) (SIF)	SMX: PEG6000 (1:9) (SGF)	SMX: Soluplus® (1:9) (SIF)
	SMX: PEG6000 (1:9) (SIF)	SMX: Soluplus® (1:9) (SIF)	SMX: PEG6000 (1:9) (SGF)	SMX: Soluplus® (1:9) (SGF)	SMX: PEG6000 (1:9) (SGF)	SMX: Soluplus® (1:9) (SGF)	SMX: PEG6000 (1:9) (SGF)	SMX: Soluplus® (1:9) (SGF)
<i>Spray dried materials</i>								
$f_2$	72.87	31.85	24.55	34.18	32.84	22.37	66.10	51.21
<i>Lyophilized materials</i>								
$f_2$	43.93	63.07	37.88	40.22	37.26	46.76	40.05	64.38

**Table 6** The release profile comparisons for NIF-polymer mixtures.

Reference material	NIF(SIF)		NIF(SGF)		NIF: Soluplus® (1:9) (SIF)	NIF: PEG6000 (1:9) (SIF)	NIF: PEG6000 (1:9) (SGF)	NIF: Soluplus® (1:9) (SIF)
	NIF: PEG6000 (1:9) (SIF)	NIF: Soluplus® (1:9) (SIF)	NIF: PEG6000 (1:9) (SGF)	NIF: Soluplus® (1:9) (SGF)	NIF: PEG6000 (1:9) (SGF)	NIF: Soluplus® (1:9) (SGF)	NIF: PEG6000 (1:9) (SGF)	NIF: Soluplus® (1:9) (SGF)
<i>Spray dried materials</i>								
$f_2$	21.76	28.93	12.11	16.21	22.85	31.68	30.47	29.12
<i>Lyophilized materials</i>								
$f_2$	15.46	21.05	7.41	5.97	20.70	22.03	29.47	18.91

reported (Khan et al., 2012; Shoaib et al., 2006). The  $n$  values were found to be 0.1929 in SIF and 0.3399 in SGF, which suggest a combination of diffusion, relaxation and erosion mechanisms.

For lyophilized SMX-PEG 6000 dispersions, the  $n$  values for drug release in SIF and SGF were found to be 0.3083 and 0.2887, respectively. A complex release mechanisms is also expected based on these  $n$  values. Also, such close  $n$  values might indicate that the medium does not substantially impact the release rate. Spray dried NIF-Soluplus® mixtures were described, rather well, using the Higuchi diffusion model. On the contrary, NIF-PEG 6000 dispersed mixtures were poorly described by all the employed release models indicating a complicated release mechanism. When release data for lyophilized NIF-Soluplus® dispersions are considered, the Higuchi and Ritger-Peppas models showed the best fit. However, the  $n$  value below 0.45 indicates mixed release mechanisms. The fit of the kinetic models to the release data indicates not only dissolution, but also diffusion, erosion, and swelling might be taking place during drug release. These potential mixed mechanisms exerted a considerable impact on drug release profiles.

#### 4.6. Comparison of release profiles

Comparison between release profiles can be executed using analysis of variance (ANOVA) between two or multiple data points (MANOVA). However, the  $f_2$ , similarity test, is usually preferable when comparing the entire dissolution release profile. Furthermore, the similarity test has been adapted by the FDA for just this sort of in vitro dissolution release profile comparison (Costa and Sousa Lobo, 2001; Polli et al., 1997).

One of the disadvantages of this method is the dependency on the dissolution profile length. It might show similarity at certain time points and dissimilarity at different time points between the same two dissolution profiles. However, the values will be hovering around 50 (Pillay and Fassihi, 1998), the cut-off for similarity of the two profiles.

The dissolution profiles were compared using this test to elucidate the impact of the selected polymer, preparation techniques, and the chosen medium, see Tables 5 and 6.

The spray dried SMX dispersion with Soluplus® or PEG 6000 exhibited a similarity in their dissolution profiles when placed in either SIF or SGF,  $f_2 = 66.10$  and 51.21, respectively. However, only the lyophilized SMX-Soluplus® dispersion showed similarity ( $f_2 = 64.38$ ) in the two release media. On the other hand, NIF dispersions did not show any similarity across the media or techniques. This suggests that the similarity that was found for SMX mixture is due to the close resemblance of SMX behavior to that of its dispersions. This is not surprising in the light of the solubility of SMX under the release conditions.

## 5. Conclusions

NIF and SMX solid dispersions were successfully prepared by spray drying and lyophilization using Soluplus® and PEG 6000. Thermal analyses showed no melting endotherm indicating the absence of crystallinity at higher polymer concentrations. Drugs dispersed in Soluplus® demonstrated a spherical shape when spray dried.

The drug dissolution rates were significantly enhanced. However, NIF dissolution rate was improved to a greater



extent due to its inherent low solubility in the two release media. Dispersions with PEG 6000 had a faster dissolution rate due to its hydrophilic nature. However, Soluplus® exhibited a tendency to maintain higher drug concentrations over time. The dissolution profiles of the different mixtures proved to be dissimilar across the preparation techniques and/or media.

### Acknowledgments

The authors are very grateful to the Deanship of Scientific Research and Research Center, College of Pharmacy, King Saud University, Riyadh, Saudi Arabia.

### References

- Abdelwahed, W., Degobert, G., Stainmesse, S., Fessi, H., 2006. Freeze-drying of nanoparticles: formulation, process and storage considerations. *Adv. Drug Deliv. Rev.* 58 (15), 1688–1713.
- Al-Obaidi, H., Buckton, G., 2009. Evaluation of griseofulvin binary and ternary solid dispersions with HPMCAS. *AAPS PharmSciTech* 10 (4), 1172–1177.
- Altamimi, M.A., Neau, S.H., 2016. Use of the Flory-Huggins theory to predict the solubility of nifedipine and sulfamethoxazole in the triblock, graft copolymer Soluplus. *Drug Dev. Ind. Pharm.* 42 (3), 446–455.
- Baird, J.A., Van Eerdenbrugh, B., Taylor, L.S., 2010. A classification system to assess the crystallization tendency of organic molecules from undercooled melts. *J. Pharm. Sci.* 99 (9), 3787–3806.
- Chan, K.L.A., Fleming, O.S., Kazarian, S.G., Vassou, D., Chrysikos, G.D., Gionis, V., 2004. Polymorphism and devitrification of nifedipine under controlled humidity: a combined FT-Raman, IR and Raman microscopic investigation. *J. Raman Spectrosc.* 35 (5), 353–359.
- Corrigan, D.O., Healy, A.M., Corrigan, O.I., 2002. The effect of spray drying solutions of polyethylene glycol (PEG) and lactose/PEG on their physicochemical properties. *Int. J. Pharm.* 235 (1), 193–205.
- Costa, P., Sousa Lobo, J.M., 2001. Modeling and comparison of dissolution profiles. *Eur. J. Pharm. Sci.* 13 (2), 123–133.
- Emara, L.H., Badr, R.M., Elbary, A.A., 2002. Improving the dissolution and bioavailability of nifedipine using solid dispersions and solubilizers. *Drug Dev. Ind. Pharm.* 28 (7), 795–807.
- Flanner, J.M.a.H., 1996. Mathematical comparison of curves with an emphasis on in-vitro dissolution profiles. *Pharm Tech.* 20 (6), 64–74.
- Forster, A.H., Tucker, J., Rades, I., 2001. The potential of small-scale fusion experiments and the gordon-taylor equation to predict the suitability of drug/polymer blends for melt extrusion. *Drug Dev. Ind. Pharm.* 27 (6), 549–560.
- Fouad, E.A., El-Badry, M., Mahrous, G.M., Alanazi, F.K., Neau, S.H., Alsarra, I.A., 2011. The use of spray-drying to enhance celecoxib solubility. *Drug Dev. Ind. Pharm.* 37 (12), 1463–1472.
- Gokturk, S., Caliskan, E., Talman, R.Y., Var, U., 2012. A study on solubilization of poorly soluble drugs by cyclodextrins and micelles: complexation and binding characteristics of sulfamethoxazole and trimethoprim. *Sci. World J.* 2012, 718791.
- Grisdale, L.C., Belton, P.S., Jamieson, M.J., Barker, S.A., Craig, D. Q., 2012. An investigation into water interactions with amorphous and milled salbutamol sulphate: the development of predictive models for uptake and recrystallization. *Int. J. Pharm.* 422 (1–2), 220–228.
- Guyot, M., Bildet, J., Bonini, F., Lagueny, A.-M., 1995. Physico-chemical characterization and dissolution of norfloxacin/cyclodextrin inclusion compounds and PEG solid dispersions. *Int. J. Pharm.* 123, 53–63.
- Hecq, J., Deleers, M., Fanara, D., Vranckx, H., Amighi, K., 2005. Preparation and characterization of nanocrystals for solubility and dissolution rate enhancement of nifedipine. *Int. J. Pharm.* 299 (1–2), 167–177.
- Homayouni, A., Sadeghi, F., Varshosaz, J., Afrasiabi Garekani, H., Nokhodchi, A., 2014. Promising dissolution enhancement effect of soluplus on crystallized celecoxib obtained through antisolvent precipitation and high pressure homogenization techniques. *Colloids Surf. B* 122, 591–600.
- Huang, J., Wigent, R.J., Bentzley, C.M., Schwartz, J.B., 2006. Nifedipine solid dispersion in microparticles of ammonio methacrylate copolymer and ethylcellulose binary blend for controlled drug delivery: effect of drug loading on release kinetics. *Int. J. Pharm.* 319 (1), 44–54.
- Huang, J., Wigent, R.J., Schwartz, J.B., 2008. Drug-polymer interaction and its significance on the physical stability of nifedipine amorphous dispersion in microparticles of an ammonio methacrylate copolymer and ethylcellulose binary blend. *J. Pharm. Sci.* 97 (1), 251–262.
- Huh, K.M., Lee, S.C., Cho, Y.W., Lee, J., Jeong, J.H., Park, K., 2005. Hydrotropic polymer micelle system for delivery of paclitaxel. *J. Control. Release* 101 (1), 59–68.
- Karavas, E., Georgarakis, E., Sigalas, M.P., Avgoustakis, K., Bikiaris, D., 2007. Investigation of the release mechanism of a sparingly water-soluble drug from solid dispersions in hydrophilic carriers based on physical state of drug, particle size distribution and drug-polymer interactions. *Eur. J. Pharm. Biopharm.* 66 (3), 334–347. official journal of Arbeitsgemeinschaft fur Pharmazeutische Verfahrenstechnik eV.
- Khan, S., Batchelor, H., Hanson, P., Saleem, I.Y., Perrie, Y., Mohammed, A.R., 2012. Dissolution rate enhancement, in vitro evaluation and investigation of drug release kinetics of chloramphenicol and sulphamethoxazole solid dispersions. *Drug Dev. Ind. Pharm.*
- Konno, H., Handa, T., Alonzo, D.E., Taylor, L.S., 2008. Effect of polymer type on the dissolution profile of amorphous solid dispersions containing felodipine. *Eur. J. Pharm. Biopharm.* 70 (2), 493–499. official journal of Arbeitsgemeinschaft fur Pharmazeutische Verfahrenstechnik eV.
- Lakshman, J.P., Cao, Y., Kowalski, J., Serajuddin, A.T., 2008. Application of melt extrusion in the development of a physically and chemically stable high-energy amorphous solid dispersion of a poorly water-soluble drug. *Mol. Pharm.* 5 (6), 994–1002.
- Law, D., Wang, W., Schmitt, E.A., Qiu, Y., Krill, S.L., Fort, J.J., 2003. Properties of rapidly dissolving eutectic mixtures of poly (ethylene glycol) and fenofibrate: the eutectic microstructure. *J. Pharm. Sci.* 92 (3), 505–515.
- Lofsson, T., Friðriksdóttir, H., Guðmundsdóttir, T.K., 1996. The effect of water-soluble polymers on aqueous solubility of drugs. *Int. J. Pharm.* 127 (2), 293–296.
- Lucida, H., Parkin, J., Sunderland, V., 2000. Kinetic study of the reaction of sulfamethoxazole and glucose under acidic conditions: I. Effect of pH and temperature. *Int. J. Pharm.* 202 (1), 47–62.
- Maa, Y.F., Nguyen, P.A., Andya, J.D., Dasovich, N., Sweeney, T.D., Shire, S.J., Hsu, C.C., 1998. Effect of spray drying and subsequent processing conditions on residual moisture content and physical/biochemical stability of protein inhalation powders. *Pharm. Res.* 15 (5), 768–775.
- Mahieu, A., Willart, J.-F., Dudognon, E., Danède, F., Descamps, M., 2012. A new protocol to determine the solubility of drugs into polymer matrixes. *Mol. Pharm.* 10 (2), 560–566.
- Mahlin, D., Bergström, C.A., 2013. Early drug development predictions of glass-forming ability and physical stability of drugs. *Eur. J. Pharm. Sci.* 49 (2), 323–332.
- Marsac, P.J., Shamblin, S.L., Taylor, L.S., 2006. Theoretical and practical approaches for prediction of drug-polymer miscibility and solubility. *Pharm. Res.* 23 (10), 2417–2426.



- Marsac, P.J., Li, T., Taylor, L.S., 2009. Estimation of drug-polymer miscibility and solubility in amorphous solid dispersions using experimentally determined interaction parameters. *Pharm. Res.* 26 (1), 139–151.
- Nagy, Z.K., Balogh, A., Vajna, B., Farkas, A., Patyi, G., Kramarics, A., Marosi, G., 2012. Comparison of electrospun and extruded Soluplus(R)-based solid dosage forms of improved dissolution. *J. Pharm. Sci.* 101 (1), 322–332.
- Ning, X., Sun, J., Han, X., Wu, Y., Yan, Z., Han, J., He, Z., 2011. Strategies to improve dissolution and oral absorption of glimepiride tablets: solid dispersion versus micronization techniques. *Drug Dev. Ind. Pharm.* 37 (6), 727–736.
- Özdemir, N., Erkin, J., 2012. Enhancement of dissolution rate and bioavailability of sulfamethoxazole by complexation with  $\beta$ -cyclodextrin. *Drug Dev. Ind. Pharm.* 38 (3), 331–340.
- Pillay, V., Fassihi, R., 1998. Evaluation and comparison of dissolution data derived from different modified release dosage forms: an alternative method. *J. Control. Release* 55 (1), 45–55.
- Polli, J.E., Rekh, G.S., Augsburger, L.L., Shah, V.P., 1997. Methods to compare dissolution profiles and a rationale for wide dissolution specifications for metoprolol tartrate tablets. *J. Pharm. Sci.* 86 (6), 690–700.
- Ruan, L.-P., Yu, B.-Y., Fu, G.-M., Zhu, D.-n., 2005. Improving the solubility of amelopisin by solid dispersions and inclusion complexes. *J. Pharm. Biomed. Anal.* 38 (3), 457–464.
- Sathigari, S.K., Radhakrishnan, V.K., Davis, V.A., Parsons, D.L., Babu, R.J., 2012. Amorphous-state characterization of efavirenz-polymer hot-melt extrusion systems for dissolution enhancement. *J. Pharm. Sci.* 101 (9), 3456–3464.
- Save, T., Venkitachalam, P., 1992. Studies on solid dispersions of nifedipine. *Drug Dev. Ind. Pharm.* 18 (15), 1663–1679.
- Sawhney, A.S., Pathak, C.P., Hubbell, J.A., 1993. Bioerodible hydrogels based on photopolymerized poly (ethylene glycol)-copoly (alpha-hydroxy acid) diacrylate macromers. *Macromolecules* 26 (4), 581–587.
- Shamma, R.N., Basha, M., 2013. Soluplus®: A novel polymeric solubilizer for optimization of Carvedilol solid dispersions: formulation design and effect of method of preparation. *Powder Technol.* 237, 406–414.
- Shoaib, M.H., Tazeen, J., Merchant, H.A., Yousuf, R.I., 2006. Evaluation of drug release kinetics from ibuprofen matrix tablets using HPMC. *Pak. J. Pharm. Sci.* 19 (2), 119–124.
- Takasuka, M., Nakai, H., 2001. IR and Raman spectral and X-ray structural studies of polymorphic forms of sulfamethoxazole. *Vib. Spectrosc.* 25 (2), 197–204.
- Tanno, F., Nishiyama, Y., Kokubo, H., Obara, S., 2004. Evaluation of hypromellose acetate succinate (HPMCAS) as a carrier in solid dispersions. *Drug Dev. Ind. Pharm.* 30 (1), 9–17.
- Tao, T., Zhao, Y., Wu, J., Zhou, B., 2009. Preparation and evaluation of itraconazole dihydrochloride for the solubility and dissolution rate enhancement. *Int. J. Pharm.* 367 (1–2), 109–114.
- Van den Mooter, G., Augustijns, P., Bleton, N., Kinget, R., 1998. Physico-chemical characterization of solid dispersions of temazepam with polyethylene glycol 6000 and PVP K30. *Int. J. Pharm.* 164 (1), 67–80.
- Vijaya Chamundeeswari, S.P., James Jebaseelan Samuel, E., Sundaraganesan, N., 2014. Molecular structure, vibrational spectra, NMR and UV spectral analysis of sulfamethoxazole. *Spectrochim. Acta Part A Mol. Biomol. Spectrosc.* 118, 1–10.
- Vijaya Kumar, S.G., Mishra, D.N., 2006. Preparation, characterization and in vitro dissolution studies of solid dispersion of Meloxicam with PEG 6000. *Yakugaku Zasshi* 126 (8), 657–664.
- Vippagunta, S.R., Wang, Z., Hornung, S., Krill, S.L., 2007. Factors affecting the formation of eutectic solid dispersions and their dissolution behavior. *J. Pharm. Sci.* 96 (2), 294–304.
- Vlassios Andronis, M.Y., George, Zograf, 1996. Effect of sorbed water on the crystallization of indomethacin from the amorphous state. *J. Pharm. Sci.* 86 (3), 346–351.
- Watson, D.G., 2005. *Pharmaceutical Analysis*. Elsevier's Health Sciences, Philadelphia, PA, USA.
- Weuts, I., Van Dycke, F., Voorspoels, J., De Cort, S., Stokbroekx, S., Leemans, R., Brewster, M.E., Xu, D., Segmuller, B., Turner, Y.T., Roberts, C.J., Davies, M.C., Qi, S., Craig, D.Q., Reading, M., 2011. Physicochemical properties of the amorphous drug, cast films, and spray dried powders to predict formulation probability of success for solid dispersions: etravirine. *J. Pharm. Sci.* 100 (1), 260–274.
- Witold, B.R.C., Ioannis, M.K., Aglaia, V., 2008. Prediction of glass transition temperatures: binary blends and copolymers. *Mater. Lett.* 62 (17–18), 3152–3155.
- Yu, H., Xia, D., Zhu, Q., Zhu, C., Chen, D., Gan, Y., 2013. Supersaturated polymeric micelles for oral cyclosporine A delivery. *Eur. J. Pharm. Biopharm.* 85 (3, Part B), 1325–1336.
- Zendelovska, D., Simeska, S., Sibinovska, O., Kostova, E., Miloševska, K., Jakovski, K., Jovanovska, E., Kikerkov, I., Trojačanec, J., Zafirov, D., 2006. Development of an HPLC method for the determination of nifedipine in human plasma by solid-phase extraction. *J. Chromatogr. B* 839 (1–2), 85–88.
- Zhang, X., Anderson, J.W., Fedida, D., 1997. Characterization of nifedipine block of the human heart delayed rectifier, hKv1.5. *J. Pharmacol. Exp. Ther.* 281 (3), 1247–1256.